American Society of Hematology
2021 L Street NW, Suite 900,
Washington, DC 20036
Phone: 202-776-0544 | Fax 202-776-0545
editorial@hematology.org

TARGETING FLT3 BY NEW-GENERATION ANTIBODY-DRUG-CONJUGATE IN COMBINATION WITH KINASE INHIBITORS FOR TREATMENT OF AML

Tracking no: BLD-2021-015246R1

Maike Roas (LMU Klinikum, Germany) Binje Vick (German Cancer Consortium (DKTK), Germany) Marc-André Kasper (Chemical Biology, Leibniz-Forschungsinstitut für Molekulare Pharmakologie, Germany) Marina Able (LMU Klinikum, Germany) Harald Polzer (LMU Klinikum, Germany) Marcus Gerlach (Tubulis GmbH, Germany) Elisabeth Kremmer (LMU münchen, Germany) Judith Hecker (German Cancer Consortium (DKTK), Germany) Saskia Schmitt (Tubulis GmbH, Germany) Andreas Stengl (LMU Munich, Germany) Verena Waller (LMU Munich, Germany) Natascha Hohmann (LMU Klinikum, Germany) Moreno Festini (LMU Klinikum, Germany) Alexander Ludwig (LMU Klinikum, Germany) Lisa Rohrbacher (Gene Center Munich, LMU, Germany) Tobias Herold (University Hospital, LMU Munich, Germany) Marion Subklewe (Gene Center Munich, LMU, Germany) Katharina Götze (German Cancer Consortium (DKTK), Germany) Christian Hackenberger (Leibniz-Forschungsinstitut für Molekulare Pharmakologie, Germany) Dominik Schumacher (Chemical Biology, Leibniz-Forschungsinstitut für Molekulare Pharmakologie, Germany) Jonas Helma-Smets (LMU Munich, Germany) Irmela Jeremias (German Cancer Consortium (DKTK), Germany) Heinrich Leonhardt (LMU Munich, Germany) Karsten Spiekermann (University Hospital Munich (LMU), Germany)

Abstract:
Fms like tyrosine kinase 3 (FLT3) is often overexpressed or constitutively activated by internal tandem duplication (ITD) and tyrosine kinase domain (TKD) mutations in acute myeloid leukemia (AML). Despite the use of receptor tyrosine kinase inhibitors (TKI) in FLT3-ITD positive AML, the prognosis of patients is still poor and further improvement of therapy is required. Targeting FLT3 independent of mutations by antibody‐drug‐conjugates (ADCs) is a promising strategy for AML therapy. Here, we report the development and preclinical characterization of a novel FLT3‐targeting ADC, 20D9-ADC, which was generated by applying the innovative P5 conjugation technology. *In vitro*, 20D9‐ADC mediated potent cytotoxicity to Ba/F3 cells expressing transgenic FLT3 or FLT3-ITD, to AML cell lines and to FLT3-ITD positive patient derived xenograft AML cells. *In vivo*, 20D9‐ADC treatment led to a significant tumor reduction and even durable complete remission in AML xenograft models. Further, 20D9‐ADC demonstrated no severe hematotoxicity in *in vitro* colony formation assays using concentrations that were cytotoxic in AML cell line treatment. The combination of 20D9-ADC with the TKI midostaurin showed strong synergy *in vitro* and *in vivo*, leading to reduction of aggressive AML cells below the detection limit. Our data indicate that targeting FLT3 with an advanced new-generation ADC is a promising and potent antileukemic strategy, especially when combined with FLT3-TKI in FLT3‐ITD positive AML.

Conflict of interest: COI declared - see note

COI notes: H.L., J.H-S., D.S., C.P.R.H. are CO-Founder of Tubulis GmbH. M.A.K., S.S. and M.G. are employees at Tubulis GmbH. M.S. received honoraria from AMGEN, BMS, Janssen, Kite/Gilead, Roche, Novartis, Pfizer, Celgene and Takeda. M.S. received research support from AMGEN, BMS, Janssen, Kite/Gilead, Miltenyi, MorphoSys, Novartis, Roche and Seattle Genetics for work unrelated to the manuscript. M.S. declare consultancy for Novartis, Janssen, AMGEN, Celgene, Kite/Gilead and Takeda. The presented work is part of a pending patent application.

Preprint server: No;

Author contributions and disclosures: K.S., H.P. and M.R. conceived the project. M.R. designed and performed experiments, analyzed and interpreted the data, wrote the manuscript and prepared the figures. E.K. generated the monoclonal antibodies, A.S. chimerized the antibody sequences. H.P., V.W., M.G., S.S., J.S.H, M.A. performed experiments. N.H., M.F, L.R. and A.L. supported the experiments. T.H. provided expression data. C.P.R.H. and M.A.K. provided and performed the antibody conjugations. I.J. and B.V. supervised and interpreted mouse experiments and generated transgenic PDX models. H.L., J.H-S. and D.S. interpreted the data and supported the project plan development. K.S. interpreted the data and coordinated the teams and experiments. C.P.R.H., M.A.K, I.J., B.V., M.S. and K.S.G. supported by interpreting the data. All authors reviewed the manuscript.

Non-author contributions and disclosures: No;

Agreement to Share Publication-Related Data and Data Sharing Statement: For original data, please contact karsten.spiekermann@med.uni-muenchen.de.

Clinical trial registration information (if any):

TARGETING FLT3 BY NEW-GENERATION ANTIBODY-DRUG-CONJUGATE IN COMBINATION WITH KINASE INHIBITORS FOR TREATMENT OF AML

Maike Roas[1-4], Binje Vick[2,5], Marc-Andre Kasper[6-8], Marina Able[1], Harald Polzer[1-3], Marcus Gerlach[8], Elisabeth Kremmer[9], Judith S. Hecker[2,3,10], Saskia Schmitt[8], Andreas Stengl[4], Verena Waller[4], Natascha Hohmann[1], Moreno Festini[1], Alexander Ludwig[1], Lisa Rohrbacher[1,11], Tobias Herold[1-3], Marion Subklewe[1,2,11], Katharina S. Götze[2,3,10,12], Christian P. R. Hackenberger[6,7], Dominik Schumacher[6-8], Jonas Helma-Smets[4,8], Irmela Jeremias[2,5,13*], Heinrich Leonhardt[4,8*] and Karsten Spiekermann[1-3,12*]

[1]Department of Medicine III, University Hospital, LMU Munich, Munich, Germany; [2]German Cancer Consortium (DKTK), Partner Site Munich, Germany; [3]German Cancer Research Centre (DKFZ), Heidelberg, Germany; [4]Department of Biology II, Human Biology and BioImaging, LMU Munich, Munich, Germany; [5]Research Unit Apoptosis in Hematopoietic Stem Cells (AHS), Helmholtz Zentrum München, German Research Center for Environmental Health (HMGU), Munich, Germany; [6]Chemical Biology, Leibniz-Forschungsinstitut für Molekulare Pharmakologie, Campus Berlin, Berlin, Germany; [7]Department of Chemistry, Humboldt Universität zu Berlin, Berlin, Germany; [8]Tubulis GmbH, Munich, Germany; [9]Institute of Molecular Immunology, Helmholtz Zentrum München, German Research Center for Environmental Health, Core Facility Monoclonal Antibodies, Munich, Germany; [10]Department of Medicine III, Technical University of Munich (TUM), Klinikum rechts der Isar, Munich, Germany; [11]Department of Translational Cancer Immunology, Gene Center Munich, LMU Munich, Munich, Germany; [12]Bavarian Cancer Research Center (BZKF); [13]Department of Pediatrics, Dr. von Hauner Children's Hospital, LMU Munich, Munich, Germany.

*These authors contributed equally to this work.

Correspondence: Karsten Spiekermann, Medizinische Klinik und Poliklinik III, Marchioninistraße 15, 81377 München; e-mail: karsten.spiekermann@med.uni-muenchen.de

Word count: 3986

Abstract word count: 216

Number of figures: 6

Number of Tables: 0

Number of references: 60

Running title: FLT3 specific ADC for AML treatment

Key Points:

FLT3 is a promising target for ADCs in AML therapy

Combination with midostaurin enhances the effectivity of FLT3-ADC in FLT3-ITD mutated AML

Abstract

Fms like tyrosine kinase 3 (FLT3) is often overexpressed or constitutively activated by internal tandem duplication (ITD) and tyrosine kinase domain (TKD) mutations in acute myeloid leukemia (AML). Despite the use of receptor tyrosine kinase inhibitors (TKI) in FLT3-ITD positive AML, the prognosis of patients is still poor and further improvement of therapy is required. Targeting FLT3 independent of mutations by antibody-drug-conjugates (ADCs) is a promising strategy for AML therapy. Here, we report the development and preclinical characterization of a novel FLT3-targeting ADC, 20D9-ADC, which was generated by applying the innovative P5 conjugation technology. *In vitro*, 20D9-ADC mediated potent cytotoxicity to Ba/F3 cells expressing transgenic FLT3 or FLT3-ITD, to AML cell lines and to FLT3-ITD positive patient derived xenograft AML cells. *In vivo*, 20D9-ADC treatment led to a significant tumor reduction and even durable complete remission in AML xenograft models. Further, 20D9-ADC demonstrated no severe hematotoxicity in *in vitro* colony formation assays using concentrations that were cytotoxic in AML cell line treatment. The combination of 20D9-ADC with the TKI midostaurin showed strong synergy *in vitro* and *in vivo,* leading to reduction of aggressive AML cells below the detection limit. Our data indicate that targeting FLT3 with an advanced new-generation ADC is a promising and potent antileukemic strategy, especially when combined with FLT3-TKI in FLT3-ITD positive AML.

Introduction

Acute myeloid leukemia (AML) is characterized by uncontrolled growth of differentiation arrested hematopoietic stem and progenitor cells. The 5-year survival rate in the US is 29.5 % (SEER data, 2011-2017), which shows the high medical need to improve therapy[1–5]. Approaches to increase efficacy of the standard 7+3 chemotherapy include the combination with targeting agents such as receptor tyrosine kinase (RTK) inhibitors (TKI) midostaurin and gilteritinib and gemtuzumab-ozogamicin (GO), an antibody drug conjugate (ADC) against CD33[6,7]. ADCs combine the specificity of antibodies with a highly potent drug[8,9] and the mechanism of action include binding to the target, internalizing and releasing the payload to kill the target cells[10]. Currently, several ADCs are investigated in preclinical settings for AML treatment, targeting for example CLL-1, CD123, IL3RA, or CXCR4 and fms like tyrosine kinase 3 (FLT3)[11–16]. The latter is

a member of the class III protein RTK and represents an established receptor for targeted therapies[17]. The binding of the FLT3-ligand induces phosphorylation, internalization and activation of downstream targets involved in survival and expansion of hematopoietic cells[18]. In healthy tissue, FLT3 cell surface expression is restricted to granulocytes/macrophage progenitors, a subset of hematopoietic stem cells (HSCs) and differentiated monocytes, dendritic cells and natural killer cells[18–21]. Remarkably, FLT3 is expressed on blasts and leukemic stem cells of most AML patients. The expression levels are significantly higher compared to healthy tissue, and high levels of FLT3 were reported as risk factor in prognosis[22,23]. Further, activating internal tandem duplication (ITD) mutations are among the most frequent genetic abnormalities in AML and occur in around 30 % of patients at diagnosis. FLT3-ITD is associated with a high risk of relapse and a poor clinical outcome[24–27]. FLT3 targeting agents, like midostaurin, are successfully applied in AML treatment[28].

Here, we report the development of a novel mutation independent FLT3 targeting ADC for AML treatment and provide proof of concept of its efficacy in preclinical *in vitro* and *in vivo* models. Recently, we have shown that the treatment of FLT3-ITD mutated AML cells with the TKI quizartinib led to an increased FLT3 expression[29]. Accordingly, a combination with FLT3-TKIs improved the efficacy of the FLT3-ADC both *in vitro* and *in vivo*.

Methods

Cell lines

Cell lines (Supplementary Table 1) were cultured according to the supplier's recommendations. For stable recombinant protein expression, Ba/F3 cells were retrovirally transduced as described before[30].

Primary samples

Primary AML samples were obtained within trials AMLCG-99 (NCT00266136) and AMLCG-2008 (NCT01382147). Healthy bone marrow samples were obtained and isolated as described before[31]. The study was performed in accordance with the ethical standards of the responsible committee on human experimentation (approval number LMU 068-08, LMU 222-10 and TUM 538/16) and with the Helsinki Declaration of 1975, as revised in 2013.

Binding and internalization of monoclonal antibodies

For antibody binding studies, cells were stained on ice with primary mouse, rat or human anti-FLT3 antibodies (in house) and secondary antibody goat $F(ab')_2$ anti-human Ig-PE (2012-09), goat anti-mouse IgG(H+L)-PE (1032-09) or goat anti-rat IgG(H+L)-PE (3052-09) purchased from

Southern Biotech. For internalization experiments, cells incubated with anti-FLT3 antibodies were washed and incubated for 30 min at 4 °C or 37 °C followed by staining with secondary antibody.

Cytotoxicity proliferation assays

Suspension cells were treated with 20D9-ADC or IgG1-ADC (in-house), deglycosylated ADC generated by applying Endo S (P0741L NEB), 20D9 mab (in house), palivizumab (404770, AbbVie), quizartinib (S1526, Selleck Chem) or midostaurin (MedChemExpress). AML cells were treated once (d 0) and viability was determined after 96 h using resazurin solution (50 µM final concentration, 4 h incubation) (R12204, Thermo Fisher Scientific). For Ba/F3 cell assays, cells were treated once (d 0) and viable cells were counted after 72 h on Vi-Cell Cell Viability Analyzer (Beckman Coulter, Krefeld, Germany). Calculation of IC_{50} values was performed using GraphPad Prism version 6.07 (GraphPad Software, La Jolla, CA, USA).

***In vivo* experiments**

Patient-derived xenograft (PDX) cells or MOLM-13 cells expressing enhanced firefly luciferase (luc) and mCherry (Addgene, Plasmid #104833) were established as described previously[32]. For *in vivo* therapy trials, luc+ MOLM-13 cells or luc- or luc+ PDX cells were injected intravenously (i.v.) into 8–12-week-old male NSG mice (NOD scid gamma, The Jackson Laboratory, Bar Harbour, ME, USA), and tumor growth was regularly monitored by blood analysis or bioluminescence imaging (BLI)[32]. After successful engraftment, mice were treated with deglycosylated or native 20D9-ADC (1 or 3 mg/kg, i.v., 1 dose per week), IgG1-ADC (3 mg/kg), or midostaurin (SelleckChem, 50 mg/kg, oral gavage, 5 doses per week; in 5 % DMSO+45 % PEG300+50 % ddH_2O). Experimental endpoints were BLI values above $1x10^{10}$ Photons/sec or below detection limit ($4x10^6$ Photons/sec) for 90-150 days post injection, or blood values above 45 % hCD45+ hCD33+ cells. Mice showing clinical signs of illness or weight loss above 15 % under therapy were sacrificed (1 ADC treated mouse in Figure 4D). Mice which died in inhalation narcosis were excluded from further analysis (1 ADC treated mouse in Figure 4D).

All animal trials were performed in accordance with the current ethical standards (Regierung von Oberbayern, number ROB-55.2Vet-2532.Vet_02-16-7).

Further information is provided in the supplementary methods.

For original data, please contact karsten.spiekermann@med.uni-muenchen.de.

Results

Generation and characterization of anti-FLT3 antibodies

FLT3 specific monoclonal antibodies (mabs) were generated by hybridoma cells of isolated B cells from immunized rats and mice. After selection procedures, seven antibodies were chimerized using a human IgG1 sequence (Supplementary Figure 1A). This antibody scaffold maintains the ability to interact with Fc gamma receptors (FcgRs), especially the high affinity variant FcgR1 (CD64), which is also expressed on AML blasts and was already evaluated for targeted therapy[33–35]. Chimeric antibodies were efficiently expressed in HEK293-F cells (Supplementary Figure 1B) and possessed high protein stability (Supplementary Figure 1C). Binding affinities to recombinant FLT3 protein varied from K_D = 11.5 ng/ml to K_D = 3981 ng/ml between the different clones (Figure 1A). Epitope mapping of the antibodies to peptides derived from extracellular domain of FLT3 identified two main binding motifs KSSSYPM (bound by 30B12, 29H1, 27E7, 20D9) and SQGESCK (bound by 19H5, 4B12, 2F12) (Figure 1B, Supplementary Figure 1D). The 20D9 showed additional affinity to a third minor epitope DGYP.

To identify their suitability for ADC development, the binding and internalization efficiencies of the antibodies to Ba/F3 cells stably expressing human wildtype FLT3 (hFLT3wt) or empty MSCV-IRES-YFP (pMIY) vector (ev) were evaluated. The clones 20D9, 4B12, 29H1 and 27E7 specifically bound the Ba/F3-hFLT3wt cells as analyzed by flow cytometry (Figure 1C and negative control in Supplementary Figure 1E) and 20D9 showed specific binding to Ba/F3 cells expressing human FLT3-ITD (hFLT3ITD) (Figure 1D, receptor expression in Supplementary Figure 1F) and/or TKD mutated FLT3 (Supplementary Figure 1G, receptor expression in Supplementary Figure 1H, Supplementary Results). Further, the antibodies displayed significant internalization of around 80 % in flow cytometry-based internalization assays in the Ba/F3-hFLT3wt cells (Figure 1C, Supplementary Figure 2A). These observations could be confirmed in FLT3+ AML cell lines in flow cytometry and immunofluorescence staining (Figure 1E, Supplementary Figure 2B,C). Further, the internalized antibodies were localized to early endosomes, which was demonstrated by the co-localization with EEA1 (Supplementary Figure 2D).

Based on internalization and high expression yields, we selected the 20D9 clone for further development and evaluated the binding to FLT3 orthologs from different species. The protein sequence of human FLT3 in epitope 1 is identical to the cynomolgus FLT3 (cynoFLT3) and differs from the murine FLT3 (mFLT3) receptor (Supplementary Figure 3A). In contrast to the mFLT3, the cynoFLT3 expressing Ba/F3 cells bound the 20D9 mab (Figure 1F, receptor

expression in Supplementary Figure 3B,C). To proof the epitope specificity, we expressed a human FLT3 receptor with the epitope region mutated to the murine variant (FLT3 S50P/P54R) in Ba/F3 cells (Supplementary Figure 3D), which did not bind the 20D9 mab (Figure 1G, Supplementary Figure 3E). Finally, we verified the binding of 20D9 mab to the high affinity Fc receptor CD64 via the IgG1 backbone using Ba/F3 cells expressing human CD64 (Figure 1H, Supplementary Figure 3F).

Generation and characterization of 20D9 antibody-drug-conjugate

We applied the P5-technology, which uses ethynylphosphonamidates for a stable conjugation to the antibodies' cysteine residues[36,37]. We conjugated IgG1-based 20D9 with the tubulin polymerization inhibitor monomethyl auristatin F (MMAF) payload with a drug to antibody ratio (DAR) of 6.2 (Figure 2A). Incubation for 2 weeks at 40 °C or storage for 14 months at 4°C did not reduce the antibody-toxin conjunction (Supplementary Figure 4A,B) and only slightly induced the aggregation (Supplementary Figure 4C,D). Furthermore, to obtain an IgG1-ADC only possessing the CD64 but no FLT3 binding, we conjugated MMAF to the IgG1 based antibody palivizumab, which is specific for the glycoprotein F of the respiratory syncytial virus[38].

In cytotoxicity assays, hFLT3wt, hFLT3ITD and hFLT3 TKD mutants (Figure 2B, Supplementary Figure 4E,F,G; Supplementary Results) as well as cynoFLT3 (Figure 2C, Supplementary Figure 4H) expressing Ba/F3 cells were sensitive to 20D9-ADC treatment. Consistent with the binding analysis, 20D9-ADC was not cytotoxic in Ba/F3-mFLT3 or epitope mutant Ba/F3-hFLT3 S50P/P54R cells (Figure 2C,D). As controls we tested the cytotoxicity of MMAF and control IgG1-ADC in Ba/F3 cells expressing the empty vector or hFLT3wt. MMAF killed Ba/F3 cells only at high concentrations and independent of FLT3 expression, while IgG1-ADC had no effect on Ba/F3 cell viability at all (Supplementary Figure 4I,J).

Further, we assessed the cytotoxicity mediated by the IgG1-FcgR binding of the 20D9-ADC. Ba/F3 cells expressing hCD64 were sensitive to 20D9-ADC and IgG1-ADC with similar mean IC_{50} of 37.3 ng/ml and 31.8 ng/ml, respectively (Figure 2E,F), while Ba/F3 cells expressing hCD16 or hCD32 did not respond to 20D9-ADC (Supplementary Figure 4K). Ba/F3 cells expressing both hFLT3wt and hCD64 (Supplementary Figure 4L) were significantly more sensitive to 20D9-ADC compared to IgG1-ADC (IC_{50}= 0.5 ng/ml versus 78.3 ng/ml), indicating the advantage of targeting both antigens *in vitro* (Figure 2F,G).

***In vitro* cytotoxic activity of 20D9-ADC in AML cell lines**

We determined the expression levels of FLT3 and CD64 in different leukemia and lymphoma cell lines (Supplementary Figure 5A,B) and could detect a significant correlation (Figure 3A). Binding of the 20D9 antibody (Supplementary Figure 5C) and cytotoxicity of the 20D9-ADC could be shown in all FLT3 positive cell lines with IC_{50} values varying between 1.3 ng/ml and 107.33 ng/ml (Figure 3B, Supplementary Table 1). Further, a TP53 knockdown in FLT3 positive AML cell lines only slightly altered IC_{50} of 20D9-ADC and FLT3 expression (Supplementary Figure 5D,E,F), indicating that a TP53 mutation is not likely to compromise efficacy.

The 20D9-ADC acts via apoptosis induction, which was demonstrated in FLT3-ITD positive MOLM-13 cells compared to FLT3 negative HL-60 cells (Supplementary Figure 5G). Further, we observed no cytotoxicity of 20D9-ADC to 5 out of 6 FLT3 negative AML cell lines. The FLT3 negative, CD64 positive cell line U-937 showed an IC_{50} of 334 ng/ml (Figure 3C). Consistently, there was a correlation of summarized CD64 and FLT3 expression and the 20D9-ADC IC_{50} (Figure 3D).

The IgG1-ADC showed cytotoxic activity in all CD64 positive cell lines (Figure 3E). The IC_{50} ranged from 12.82 to around 2000 ng/ml and were noticeably higher compared to the 20D9-ADC (Supplementary Table 1). FLT3 positive and negative cell lines showed similar sensitivity towards the payload MMAF (Supplementary Figure 5H). The native 20D9 antibody or the IgG1 antibody did not impair cell proliferation (Supplementary Figure 5I and data not shown).

To investigate the impact of CD64 interaction on the efficacy of IgG1 based ADCs, we disrupted the CD64-IgG1 binding by removing the N-linked glycans of 20D9-ADC and IgG1-ADC (Supplementary Figure 5J). Compared to the native 20D9-ADC, the IC_{50} of deglycosylated 20D9-ADC shifted from 15.7 ng/ml to 473.7 ng/ml reflecting the proportions of FLT3 and CD64 specific targeting. As control, the deglycosylated IgG1-ADC showed no activity on MOLM-13 cells, confirming the effective abrogation of the CD64-FcgR interaction (Figure 3F).

Antileukemic activity of 20D9-ADC in cell line and patient-derived xenograft AML mouse models

To determine the *in vivo* antileukemic activity of 20D9-ADC, we transplanted MOLM-13 or patient derived xenograft (PDX) cells into NSG mice. For sensitive monitoring of tumor burden by bioluminescent imaging (BLI), luciferase-expressing cells were used which showed similar FLT3 expression levels than parental cells (Supplementary Figure 6A).

First, we analyzed the efficacy of ADCs on MOLM-13 cells *in vivo*. While repetitive administration of 1 mg/kg (Q1Wx6) 20D9-ADC decelerated the increase of tumor burden compared to PBS

237 treated mice, 3 mg/kg (Q1Wx4) led to a strong reduction of tumor burden below detection limit
238 for at least 154 days (Figure 4A,B). The effect was comparable if therapy started at intermediate
239 or advanced tumor burden (Supplementary Figure 6B). To define CD64-related effects, we
240 applied native and deglycosylated IgG1-ADC and 20D9-ADC. Interestingly, the deglycosylated
241 20D9-ADC showed strong cytotoxicity comparable to the native 20D9-ADC, indicating that FLT3
242 targeting is sufficient to elicit a long-lasting response. In contrast, the effect of native IgG1-ADC
243 (3 mg/kg; Q1Wx2) was reduced compared to native 20D9-ADC underlining that CD64 targeting
244 was less effective *in vivo.* The deglycosylated IgG1-ADC had only a minimal effect compared to
245 PBS treatment, confirming the functional abrogation of CD64-IgG1 interaction (Figure 4C).

246 Next, we determined the effect of 20D9-ADC on native and luciferase positive PDX samples[32]. We
247 selected samples with FLT3-ITD mutation and moderate to high FLT3 expression compared to
248 AML patient samples[39] (Figure 4D, Supplementary Table 2). *Ex vivo*, the PDX cells were sensitive
249 to 20D9-ADC treatment but not to 20D9 mab treatment (Supplementary Figure 6C,D). *In vivo*
250 treatment of AML-573 transplanted mice with 3 mg/kg 20D9-ADC (Q1Wx5) led to a strong
251 tumor reduction followed by stable low tumor burden up to 150 days, both if treatment started
252 at intermediate or at advanced tumor burden (Figure 4E,F). The strong effect of 20D9-ADC could
253 also be seen when native primograft AML-573 cells were transplanted (Supplementary Figure
254 6E). Similarly, in two additional PDX samples, AML-640 and AML-579, treatment with 3 mg/kg
255 20D9-ADC (Q1Wx3) at intermediate or advanced tumor burden led to a strong tumor reduction
256 followed by a tumor outgrowth after treatment stop (Supplementary Figure 6F-I).

257

258 **Hematotoxicity of 20D9-ADC**

259 To assess hematotoxicity, we investigated the effect of 20D9-ADC on normal human
260 hematopoietic cells *in vitro* by analyzing bone marrow cells from healthy donors enriched for
261 CD34+ cells (Supplementary Figure 7A,B). As expected, FLT3 expression could be detected in
262 18.9 % ± 2.9 % of CD34+ cells, while CD64 was barely expressed (1 % ± 0.6 %, Figure 5A). Cells
263 were treated with ADC concentrations within the range of the observed IC_{50} in AML cells (40 and
264 200 ng/ml) and with high dose (1000 ng/ml). Only treatment with the high dose of both
265 20D9-ADC and IgG1-ADC led to a significant decrease in cell viability (Figure 5B) and might
266 indicate IgG1-dependent toxicity that induces a significant reduction of CD64 expressing cells
267 after treatment (Supplementary Figure 7C). Accordingly, an effect on the differentiation capacity
268 could only be seen after treatment with high dose 20D9-ADC, which revealed a significantly
269 decreased proportion of HSC, CD34+CD38-, CD34+CD38+, multi-lymphoid progenitor (MLP),
270 common myeloid progenitor (CMP), and granulocyte-monocyte progenitor (GMP) cell
271 populations (Figure 5C). After treatment with IgG1-ADC, we observed significantly decreased

MLPs, CMPs, and GMPs but to a lower extent compared to the 20D9-ADC. Furthermore, we assessed clonogenic capacity by colony forming unit assay of healthy CD34+ cells (Figure 5D, Supplementary Figure 7D). Again, only high dose treatment with 20D9-ADC and IgG1-ADC revealed significantly reduced granulocytic, monocytic and granulocytic-macrophagic colony formation. The erythroid progenitors were unaffected.

Treatment combination of 20D9-ADC and TKIs

We have previously shown that TKI treatment increased the surface expression of FLT3 on FLT3-ITD positive AML cells and sensitized them to bispecific FLT3 x CD3 antibodies[29]. Thus, we combined the 20D9-ADC with TKIs for treatment of FLT3 mutated AML, to increase the cytotoxic activity of the ADC. Incubation of MOLM-13 (FLT3-ITD heterozygote), MV4-11 (FLT3-LOH-ITD) and MM-6 (V592A) cells with midostaurin, quizartinib or sorafenib led to an increase of FLT3 cell surface expression after incubation, (Figure 6A,B and Supplementary Figure 8A,B). To investigate whether this is a FLT3-TKI specific effect, we determined the FLT3 expression as response to the control TKI dasatinib, that targets BCR-ABL, c-KIT, EPH and PDGFβ and is used in CML, ALL and AML therapy[40]. Even though dasatinib exhibits similar effects on cell viability compared to FLT3 TKIs in selected concentrations (data not shown), dasatinib does not upregulate FLT3 surface expression (Figure 6B).

Different dose combinations of 20D9-ADC and TKI were applied to MOLM-13 cells *in vitro*. While midostaurin as single drug did not affect cell viability at low doses, combination treatment with the 20D9-ADC was significantly beneficial compared to 20D9-ADC treatment alone (Figure 6C). Similar effects could be observed for the combination of 20D9-ADC and AC220 in MOLM-13, MV4-11 and MM-6 cells (Figure 6E and Supplementary Figure 8C). To calculate synergistic effects, we utilized two calculation methods, the Combination Index (CI)[41,42] and the ZIP method using the Synergy finder[43,44], which revealed synergism of a combined treatment approach with 20D9-ADC and FLT3-TKI (Figure 6C-F). In the MOLM-13 xenograft model, treatment with midostaurin (50 mg/kg; Q5Wx3) or 20D9-ADC (1 mg/kg; Q1Wx3) as single agents only led to modest growth delay *in vivo* (Figure 6G). Strikingly, the combination of 20D9-ADC and midostaurin treatment led to drastic tumor reduction and probably cure in 2 out of 3 tumor-bearing animals. Thus, these results indicate a high synergistic potential of the FLT3 specific ADC when combined with FLT3 TKIs.

Discussion

Here, we report the development and preclinical characterization of a novel FLT3 targeting ADC, 20D9-ADC, with robust preclinical activity in multiple models of AML. Further, we found a strong synergistic effect of the combination treatment of 20D9-ADC with a recently approved TKI in FLT3 mutated AML.

FLT3 is an established target for TKIs, like midostaurin which are approved in FLT3 mutated AMLs with permanently activated receptor signaling[45]. Moreover, FLT3 is overexpressed in AML with a restricted expression pattern in a subset of healthy hematopoietic cells and low abundance in non-hematopoietic tissue. There, a low RNA expression in lung, pancreas and brain was not yet confirmed to result in cell surface expression of FLT3. Thus, agents targeting FLT3 in AML may have the largest therapeutic index compared to other targets like CD33, CD123 and CLL1[46] and are expected to have little to no healthy tissue toxicity beyond potential hematologic toxicities[46]. This makes FLT3 a promising ADC target in AML treatment, addressing a broader patient cohort regardless of the FLT3 mutation status.

So far, GO, an ADC targeting CD33, is the only approved ADC in AML[53,54]. The conjugation and linker design in ADC development are essential as they influence the toxicology profile[8]. The linker of GO exhibits instability, leading to premature release of calicheamycin[47]. For 20D9-ADC development, the novel P5 conjugation technology with outstanding serum stability was applied to conjugate MMAF via a cleavable linker, which facilitates efficient intracellular release of MMAF [37,48]. MMAF belongs, like monomethyl auristatin E (MMAE), to the microtubule-targeting agents which are used as payloads in two-thirds of all clinical stage ADCs[49]. It is a highly potent agent with IC_{50} in the subnanomolar range and has lower bystander killing effects in comparison to MMAE, which is an advantage in hematologic malignancies[50,51].

We show here that 20D9-ADC had strong and selective cytotoxicity in FLT3 positive cell lines *in vitro.* We could clearly distinguish between CD64- and FLT3-mediated cytotoxicity in a cell line model by applying deglycosylated ADCs, showing a strong advantage of co-targeting both receptors. *In vivo*, we found a dose dependent response of aggressive AML cell lines to 20D9-ADC independent from the tumor burden at start of treatment, proving the robustness and high efficacy of 20D9-ADC. Interestingly, the deglycosylated 20D9-ADC achieved almost the same efficacy compared to the native 20D9-ADC in MOLM-13 cells *in vivo*, despite targeting exclusively FLT3. Applying IgG1-ADC *in vivo* was much less effective than 20D9-ADC, indicating that FLT3 targeting might be sufficient and superior compared to dual targeting in the AML mouse model. Moreover, we could also successfully treat AML PDX models *in vivo*. These PDX samples recapitulate the phenotype of human AML since they comprise of AML stem cells and subclonal AML cell populations[32,52]. In the *in vivo* studies, the ADCs were well tolerated as single agent or in combination with TKIs.

To evaluate the toxicity profile of 20D9-ADC in healthy tissue, we focused on hematopoietic stem and progenitor cells, since FLT3 expression in the brain, pancreas and lung tissue seems to be limited to the cytoplasm or to be very low[46]. 20D9-ADC in concentrations in the range of IC_{50} values of AML cell lines did not affect healthy human CD34+ cells, which is promising for a favourable toxicity profile. Only in high concentrations, the 20D9-ADC but also the IgG1-ADC shows cytotoxicity towards myelomonocytic and lymphoid progenitors. Thus, Fc receptor engagement might result in side effects and toxicity toward megakaryocytes leading to thrombocytopenia[53]. On the other hand, brentuximab vedotin, an approved IgG1-based ADC in Hodgkin lymphoma, showed manageable tolerability and safety profile in a phase III study[54]. A functional IgG1 Fc region might also have advantages as it was reported that IgG1 can mediate antibody-dependent cell-mediated cytotoxicity and antibody-dependent cellular phagocytosis in the context of drug conjugates[49,55–57]. Of note, our studies have shown a superior cytotoxic activity of the native 20D9-ADC compared to the deglycosylated 20D9-ADC (that is devoid of FcgR binding) *in vitro*, but not *in vivo*. It is unclear whether the FcgR binding properties of the 20D9-ADC will be beneficial in AML patients with respect to toxicity and efficacy. Therefore, further studies in humans or nonhuman primates will be necessary to answer this question. For FLT3 targeting, a favourable toxicity profile can be expected, since a FLT3 x CD3 bispecific antibody in cynomolgues monkey revealed a reversible depletion of dendritic cells, HSPCs and monocytes without any major clinical signs of toxicity[46].

Due to the observed high efficacy, we evaluated the potential of 20D9-ADC for therapy of FLT3 mutated AML, since especially patients with a high ratio of FLT3 ITD have a worse prognosis[58]. By combining 20D9-ADC and FLT3 TKIs, we aimed at (1) exploiting the potential of the FLT3 target, since the ITD mutated FLT3 receptor has a partially intracellular localization[29], (2) opening the therapeutic window for the FLT3 specific ADC treatment while reducing side effects, and at (3) integrating an FLT3 ADC in the therapeutic landscape of FLT3-mutated AML.

The combination of 20D9-ADC and TKI treatment showed significantly higher effectivity *in vitro* compared to single drug treatment. The *in vivo* experiments resulted in even more striking benefit of the combination therapy of low dose 20D9-ADC and midostaurin. We hypothesize that the outstanding treatment efficacy of the drug combination of 20D9-ADC and midostaurin is due to an upregulation of the activated FLT3 receptor on the cell surface as previously reported by our group[29]. However, we cannot exclude other mechanisms as midostaurin is not specific for FLT3 and inhibits also other kinases like VEGFR-2, PDGFR and KIT[59]. Further, Fu Li et al described an anti CD123-ADC to be more efficient in combination with quizartinib[14] and a CD33-targeting ADC (IMGN779) showed increased effectivity in combination with quizartinib[60].

Interestingly, an anti-FLT3 ADC from Astellas Pharma (AGS62P1; NCT02864290) is being evaluated in clinical studies, supporting the relevance of the FLT3 receptor as a therapeutic target for ADCs[55]. Our study using 20D9-ADC clearly distinguishes from the AGS62P1 molecule. We (1) use Ethynylphosphonamidate-linkers with excellent stability as opposed to oxime linkages in AGS62P1, which is (2) limited to DAR2 and we believe that the expression profile of FLT3 dictates a higher DAR to ensure a good efficacy also in FLT3-low expressing malignant cells. Further, the (3) additional CD64 targeting and (4) the combination therapy with TKIs to enhance the efficacy is mostly promising regarding the effectivity in FLT3+ AML.

In conclusion, we have developed and characterized a novel FLT3 targeting ADC that demonstrated potent antileukemic activity in preclinical models of AML including PDX mouse models. Importantly, 20D9-ADC was effective at low concentrations in combination with midostaurin, suggesting a treatment concept with a possibly favorable toxicity profile. Our data indicate that FLT3 is a clinically promising target for ADC application which should be further evaluated in clinical studies in combination with FLT3 inhibitors.

Acknowledgments

We thank Belay Tizazu for generating Ba/F3 cell models and performing experiments. We thank Maike Fritschle and Annette Frank for animal handling. We thank Bianka Ksienzyk for cell sorting. We acknowledge the iFlow Core Facility of the university hospital Munich (INST 409/225-1 FUGG) for assistance with the generation of flow cytometry data. This work was supported by the German Research Foundation (DFG) to H.L., I.J., K.S. and K.S.G. (SFB 1243) and to H.L. and A.S. (SPP1623 and GRK1721) and to M.A.K. and C.P.R.H. (SPP1623) and by German Ministry of Education and Research (BMBF) to K.S., M.A. and H.L. (Project 16GW0360). C.P.R.H. and H.L. were supported by the Leibniz Association within the Leibniz Competition (SAW-2018-FMP-4-P5Label, T18/2017). K.S.G has received funding from the European Union's Horizon 2020 Marie Sklodowska-Curie Innovative Training Network (MSCA-ITN, Grant agreement 953407) and German Jose Carreras Leukämiestiftung (DJCLS grant R14). M.S. received research funding from a German Research Foundation (DFG) grant (451580403), SFB-TRR 388/1 2021-452881907, Bavarian Elite Graduate Training Network, Else-Kröner-Fresenius Stiftung and Bavarian Center for Cancer Research (BZKF). M.R. was member of the IRTG-1243 within the SFB 1243. The authors thank all study participants.

Authorship

Contributions: K.S., H.P. and M.R. conceived the project. M.R. designed and performed experiments, analyzed and interpreted the data, wrote the manuscript and prepared the figures. E.K. generated the monoclonal antibodies, A.S. chimerized the antibody sequences. H.P., V.W., M.G., S.S., J.S.H, M.A. performed experiments. N.H., M.F, L.R. and A.L. supported the experiments. T.H. provided expression data. C.P.R.H. and M.A.K. provided and performed the antibody conjugations. I.J. and B.V. supervised and interpreted mouse experiments and generated transgenic PDX models. H.L., J.H-S. and D.S. interpreted the data and supported the project plan development. K.S. interpreted the data and coordinated the teams and experiments. C.P.R.H., M.A.K, I.J., B.V., M.S. and K.S.G. supported by interpreting the data. All authors reviewed the manuscript.

Conflict-of-Interest Disclosures: H.L., J.H-S., D.S., C.P.R.H. are CO-Founder of Tubulis GmbH. M.A.K., S.S. and M.G. are employees at Tubulis GmbH. M.S. received honoraria from AMGEN, BMS, Janssen, Kite/Gilead, Roche, Novartis, Pfizer, Celgene and Takeda. M.S. received research support from AMGEN, BMS, Janssen, Kite/Gilead, Miltenyi, MorphoSys, Novartis, Roche and Seattle Genetics for work unrelated to the manuscript. M.S. declare consultancy for Novartis, Janssen, AMGEN, Celgene, Kite/Gilead and Takeda.

The presented work is part of a pending patent application.

Additional author information: The current affiliation of E.K. is Department of Biology II, LMU Munich, Munich, Germany.

Correspondence: Karsten Spiekermann, Medizinische Klinik und Poliklinik III, Marchioninistraße 15, 81377 München; e-mail: karsten.spiekermann@med.uni-muenchen.de

References

1. Acute Myeloid Leukemia — Cancer Stat Facts. Accessed June 15, 2021. https://seer.cancer.gov/statfacts/html/amyl.html

2. Shallis RM, Wang R, Davidoff A, Ma X, Zeidan AM. Epidemiology of acute myeloid leukemia: Recent progress and enduring challenges. *Blood Rev*. 2019;36:70-87. doi:10.1016/j.blre.2019.04.005

3. Döhner H, Estey E, Grimwade D, et al. Diagnosis and management of AML in adults: 2017 ELN recommendations from an international expert panel. *Blood*. 2017;129(4):424-447. doi:10.1182/blood-2016-08-733196

4. Kantarjian H, Kadia T, DiNardo C, et al. Acute myeloid leukemia: current progress and future directions. *Blood Cancer J*. 2021;11(2):41. doi:10.1038/s41408-021-00425-3

5. Herold T, Rothenberg-Thurley M, Grunwald V V., et al. Validation and refinement of the revised 2017 European LeukemiaNet genetic risk stratification of acute myeloid leukemia. *Leukemia*. 2020;34(12):3161-3172. doi:10.1038/s41375-020-0806-0

6. Carter JL, Hege K, Yang J, et al. Targeting multiple signaling pathways: the new approach to acute myeloid leukemia therapy. *Signal Transduct Target Ther*. 2020;5(1). doi:10.1038/s41392-020-00361-x

7. Stanchina M, Soong D, Zheng-Lin B, Watts JM, Taylor J. Advances in acute myeloid leukemia: Recently approved therapies and drugs in development. *Cancers (Basel)*. 2020;12(11):1-32. doi:10.3390/cancers12113225

8. Schumacher D, Hackenberger CPR, Leonhardt H, Helma J. Current Status: Site-Specific Antibody Drug Conjugates. *J Clin Immunol*. 2016;36:100-107. doi:10.1007/s10875-016-0265-6

9. Drago JZ, Modi S, Chandarlapaty S. Unlocking the potential of antibody–drug conjugates for cancer therapy. *Nat Rev Clin Oncol*. 2021;18(6):327-344. doi:10.1038/s41571-021-00470-8

10. Beck A, Goetsch L, Dumontet C, Corvaïa N. Strategies and challenges for the next generation of antibody-drug conjugates. *Nat Rev Drug Discov*. 2017;16(5):315-337. doi:10.1038/nrd.2016.268

11. Costa MJ, Kudaravalli J, Ma JT, et al. Optimal design, anti-tumour efficacy and tolerability of anti-CXCR4 antibody drug conjugates. *Sci Rep*. 2019;9(1). doi:10.1038/s41598-019-38745-x

12. Kirchhoff D, Stelte-Ludwig B, Lerchen HG, et al. Il3ra-targeting antibody–drug conjugate bay-943 with a kinesin spindle protein inhibitor payload shows efficacy in preclinical models of hematologic malignancies. *Cancers (Basel)*. 2020;12(11):1-17. doi:10.3390/cancers12113464

13. Kovtun Y, Jones G, Harvey L, et al. IMGN632: A novel antibody-drug conjugate (ADC) of a CD123-targeting antibody with a potent DNA-alkylator is highly active in preclinical models of AML with poor prognosis. *Haematologica*. 2016;101:222.

14. Li F, Sutherland MK, Yu C, et al. Characterization of SGN-CD123A, APotent CD123-directed antibody-drug conjugate for acute myeloid leukemia. *Mol Cancer Ther*. 2018;17(2):554-564. doi:10.1158/1535-7163.MCT-17-0742

15. Jiang YP, Liu BY, Zheng Q, et al. CLT030, a leukemic stem cell-targeting CLL1 antibody-drug conjugate for treatment of acute myeloid leukemia. *Blood Adv*. 2018;2(14):1738-1749. doi:10.1182/bloodadvances.2018020107

16. Rudra-Ganguly N, Lowe C, Virata C, et al. AGS62P1, a Novel Anti-FLT3 Antibody Drug Conjugate, Employing Site Specific Conjugation, Demonstrates Preclinical Anti-Tumor Efficacy in AML Tumor and Patient Derived Xenografts. *Blood*. 2015;126(23):3806-3806. doi:10.1182/blood.v126.23.3806.3806

17. Kiyoi H, Ohno R, Ueda R, Saito H, Naoe T. Mechanism of constitutive activation of FLT3 with internal tandem duplication in the juxtamembrane domain. *Oncogene*. 2002;21(16):2555-2563. doi:10.1038/sj.onc.1205332

18. Grafone T, Palmisano M, Nicci C, Storti S. An overview on the role of FLT3-tyrosine kinase receptor in acute myeloid leukemia: Biology and treatment. *Oncol Rev*. 2012;6(1):64-74. doi:10.4081/oncol.2012.e8

19. Kikushige Y, Yoshimoto G, Miyamoto T, et al. Human Flt3 Is Expressed at the Hematopoietic Stem Cell and the Granulocyte/Macrophage Progenitor Stages to Maintain Cell Survival. *J Immunol*. 2008;180(11):7358-7367. doi:10.4049/jimmunol.180.11.7358

20. Böiers C, Buza-Vidas N, Jensen CT, et al. Expression and role of FLT3 in regulation of the earliest stage of normal granulocyte-monocyte progenitor development. *Blood*.

2010;115(24):5061-5068. doi:10.1182/blood-2009-12-258756

21. Karsunky H, Merad M, Cozzio A, Weissman IL, Manz MG. Flt3 ligand regulates dendritic cell development from Flt3+ lymphoid and myeloid-committed progenitors to Flt3+ dendritic cells in vivo. *J Exp Med*. 2003;198(2):305-313. doi:10.1084/jem.20030323

22. Brauchle B, Goldstein RL, Karbowski CM, et al. Characterization of a novel FLT3 BiTE molecule for the treatment of acute myeloid leukemia. *Mol Cancer Ther*. 2020;19(9):1875-1888. doi:10.1158/1535-7163.MCT-19-1093

23. Cheng J, Qu L, Wang J, Cheng L, Wang Y. High expression of FLT3 is a risk factor in leukemia. *Mol Med Rep*. 2018;17(2):2885-2892. doi:10.3892/mmr.2017.8232

24. Schranz K, Hubmann M, Harin E, et al. Clonal heterogeneity of FLT3-ITD detected by high-throughput amplicon sequencing correlates with adverse prognosis in acute myeloid leukemia. *Oncotarget*. 2018;9(53):30128-30145. doi:10.18632/oncotarget.25729

25. Janke H, Pastore F, Schumacher D, et al. Activating FLT3 mutants show distinct gain-of-function phenotypes in vitro and a characteristic signaling pathway profile associated with prognosis in acute Myeloid Leukemia. *PLoS One*. 2014;9(3). doi:10.1371/journal.pone.0089560

26. Daver N, Schlenk RF, Russell NH, Levis MJ. Targeting FLT3 mutations in AML: review of current knowledge and evidence. *Leukemia*. 2019;33(2):299-312. doi:10.1038/s41375-018-0357-9

27. Spiekermann K, Bagrintseva K, Schwab R, Schmieja K, Hiddemann W. Overexpression and constitutive activation of FLT3 induces STAT5 activation in primary acute myeloid leukemia blast cells. *Clin Cancer Res*. 2003;9(6):2140-2150.

28. Megías-Vericat JE, Ballesta-López O, Barragán E, Martínez-Cuadrón D, Montesinos P. Tyrosine kinase inhibitors for acute myeloid leukemia: A step toward disease control? *Blood Rev*. 2020;44. doi:10.1016/j.blre.2020.100675

29. Reiter K, Polzer H, Krupka C, et al. Tyrosine kinase inhibition increases the cell surface localization of FLT3-ITD and enhances FLT3-directed immunotherapy of acute myeloid leukemia. *Leukemia*. 2018;32(2):313-322. doi:10.1038/leu.2017.257

30. Polzer H, Janke H, Schmid D, Hiddemann W, Spiekermann K. Casitas B-lineage lymphoma mutants activate AKT to induce transformation in cooperation with class III receptor tyrosine kinases. *Exp Hematol*. 2013;41(3):271-280.e4. doi:10.1016/j.exphem.2012.10.016

31. Hecker JS, Hartmann L, Rivière J, et al. CHIP & HIPs: Clonal Hematopoiesis is Common in Hip Arthroplasty Patients and Associates with Autoimmune Disease. *Blood*. Published online June 17, 2021. doi:10.1182/blood.2020010163

32. Vick B, Rothenberg M, Sandhöfer N, et al. An advanced preclinical mouse model for acute myeloid leukemia using patients' cells of various genetic subgroups and in vivo bioluminescence imaging. *PLoS One*. 2015;10(3):1-20. doi:10.1371/journal.pone.0120925

33. Dunphy CH, Tang W. The value of CD64 expression in distinguishing acute myeloid leukemia with monocytic differentiation from other subtypes of acute myeloid leukemia: A flow cytometric analysis of 64 cases. *Arch Pathol Lab Med*. 2007;131(5):748-754. doi:10.5858/2007-131-748-tvocei

34. Tur MK, Huhn M, Jost E, Thepen T, Brümmendorf TH, Barth S. In vivo efficacy of the recombinant anti-CD64 immunotoxin H22(scFv)-ETA′ in a human acute myeloid leukemia xenograft tumor model. *Int J Cancer*. 2011;129(5):1277-1282. doi:10.1002/ijc.25766

35. Mladenov R, Hristodorov D, Cremer C, et al. CD64-directed microtubule associated protein tau kills leukemic blasts ex vivo. *Oncotarget*. 2016;7(41):67166-67174. doi:10.18632/oncotarget.11568

36. Kasper MA, Glanz M, Stengl A, et al. Cysteine-Selective Phosphonamidate Electrophiles for Modular Protein Bioconjugations. *Angew Chemie - Int Ed*. 2019;58(34):11625-11630. doi:10.1002/anie.201814715

37. Kasper MA, Stengl A, Ochtrop P, et al. Ethynylphosphonamidates for the Rapid and Cysteine-Selective Generation of Efficacious Antibody–Drug Conjugates. *Angew Chemie - Int Ed*. 2019;58(34):11631-11636. doi:10.1002/anie.201904193

38. Fenton C, Scott LI, Plosker GL. Palivizumab: A review of its use as prophylaxis for serious respiratory syncytial virus infection. *Pediatr Drugs*. 2004;6(3):177-197. doi:10.2165/00148581-200406030-00004

39. Herold T, Jurinovic V, Batcha AMN, et al. A 29-gene and cytogenetic score for the prediction of resistance to induction treatment in acute myeloid leukemia. *Haematologica*. 2018;103(3):456-465. doi:10.3324/haematol.2017.178442

40. Paschka P, Schlenk RF, Weber D, et al. Adding dasatinib to intensive treatment in core-binding factor acute myeloid leukemia-results of the AMLSG 11-08 trial. *Leukemia*. 2018;32(7):1621-1630. doi:10.1038/s41375-018-0129-6

41. Chou T-C, Martin N. *CompuSyn for Drug Combinations and for General Dose-Effect Analysis User's Guide A Computer Program for Quantitation of Synergism and Antagonism in Drug Combinations, and the Determination of IC 50 , ED 50 , and LD 50 Values.*; 2005. www.combosyn.com

42. Chou TC. Theoretical basis, experimental design, and computerized simulation of synergism and antagonism in drug combination studies. *Pharmacol Rev*. 2006;58(3):621-681. doi:10.1124/PR.58.3.10

43. Yadav B, Wennerberg K, Aittokallio T, Tang J. Searching for Drug Synergy in Complex Dose-Response Landscapes Using an Interaction Potency Model. *Comput Struct Biotechnol J*. 2015;13:504-513. doi:10.1016/j.csbj.2015.09.001

44. Ianevski A, Giri AK, Aittokallio T. SynergyFinder 2.0: Visual analytics of multi-drug combination synergies. *Nucleic Acids Res*. 2021;48(1):W488-W493. doi:10.1093/NAR/GKAA216

45. Hospital MA, Green AS, Maciel TT, et al. FLT3 inhibitors: Clinical potential in acute myeloid leukemia. *Onco Targets Ther*. 2017;10:607-615. doi:10.2147/OTT.S103790

46. Yeung YA, Krishnamoorthy V, Dettling D, et al. An Optimized Full-Length FLT3/CD3 Bispecific Antibody Demonstrates Potent Anti-leukemia Activity and Reversible Hematological Toxicity. *Mol Ther*. 2020;28(3):889-900. doi:10.1016/j.ymthe.2019.12.014

47. ten Cate B, Bremer E, de Bruyn M, et al. A novel AML-selective TRAIL fusion protein that is superior to Gemtuzumab Ozogamicin in terms of in vitro selectivity, activity and stability. *Leukemia*. 2009;23(8):1389-1397. doi:10.1038/leu.2009.34

48. Kostova V, Désos P, Starck JB, Kotschy A. The chemistry behind adcs. *Pharmaceuticals*. 2021;14(5). doi:10.3390/ph14050442

49. Hoffmann RM, Coumbe BGT, Josephs DH, et al. Antibody structure and engineering considerations for the design and function of Antibody Drug Conjugates (ADCs). *Oncoimmunology*. 2018;7(3):1-11. doi:10.1080/2162402X.2017.1395127

50. Yaghoubi S, Karimi MH, Lotfinia M, et al. Potential drugs used in the antibody–drug

conjugate (ADC) architecture for cancer therapy. *J Cell Physiol*. 2020;235(1):31-64. doi:10.1002/jcp.28967

51. Ponziani S, Di Vittorio G, Pitari G, et al. Antibody-drug conjugates: The new frontier of chemotherapy. *Int J Mol Sci*. 2020;21(15):1-28. doi:10.3390/ijms21155510

52. Ebinger S, Zeller C, Carlet M, et al. Plasticity in growth behavior of patients' acute myeloid leukemia stem cells growing in mice. *Haematologica*. 2020;105(12):2855-2860. doi:10.3324/haematol.2019.226282

53. Uppal H, Doudement E, Mahapatra K, et al. Potential mechanisms for thrombocytopenia development with trastuzumab emtansine (T-DM1). *Clin Cancer Res*. 2015;21(1):123-133. doi:10.1158/1078-0432.CCR-14-2093

54. Scott LJ. Brentuximab Vedotin: A Review in CD30-Positive Hodgkin Lymphoma. *Drugs*. 2017;77(4):435-445. doi:10.1007/s40265-017-0705-5

55. Junttila TT, Li G, Parsons K, Phillips GL, Sliwkowski MX. Trastuzumab-DM1 (T-DM1) retains all the mechanisms of action of trastuzumab and efficiently inhibits growth of lapatinib insensitive breast cancer. *Breast Cancer Res Treat*. 2011;128(2):347-356. doi:10.1007/s10549-010-1090-x

56. Weiskopf K, Weissman IL. Macrophages are critical effectors of antibody therapies for cancer. *MAbs*. 2015;7(2):303-310. doi:10.1080/19420862.2015.1011450

57. Gong Q, Ou Q, Ye S, et al. Importance of Cellular Microenvironment and Circulatory Dynamics in B Cell Immunotherapy. *J Immunol*. 2005;174(2):817-826. doi:10.4049/jimmunol.174.2.817

58. Kiyoi H, Kawashima N, Ishikawa Y. FLT3 mutations in acute myeloid leukemia: Therapeutic paradigm beyond inhibitor development. *Cancer Sci*. 2020;111(2):312-322. doi:10.1111/cas.14274

59. Weisberg E, Sattler M, Manley PW, Griffin JD. Spotlight on midostaurin in the treatment of FLT3-mutated acute myeloid leukemia and systemic mastocytosis: Design, development, and potential place in therapy. *Onco Targets Ther*. Published online 2018. doi:10.2147/OTT.S127679

60. Walker R, Watkins K, Zweidler-McKay P. Combination treatment with antibody-drug-conjugates and FLT3 inhibitors PCT/US20 19/032090 Immunogen, Inc. 2019;2(51).

61. Bagnoli JW, Ziegenhain C, Janjic A, et al. Sensitive and powerful single-cell RNA sequencing using mcSCRB-seq. 2018;9(1):1-8. doi:10.1038/s41467-018-05347-6

Figure Legends

Figure 1: Evaluation of epitope specificity and internalization capability of anti-FLT3 monoclonal antibodies.

(A) Affinity of seven anti-FLT3 monoclonal antibody (mab) clones to recombinant human FLT3 measured in enzyme-linked immunosorbent assay (ELISA) normalized to the binding of the antibodies to BSA control. Dissociation constant (K_D; mean ± s.d..; n=3) is depicted. (B) Schematic FLT3 receptor. Black arrows indicate common mutations and blue arrows indicate the three identified epitopes of seven anti-FLT3 antibodies analyzed in linear epitope mapping by PEPperPRINT©. Figure was created with BioRender.com. (C) Binding and temperature induced internalization of anti-FLT3 antibodies in Ba/F3 cells expressing human wildtype FLT3. Internalization was induced by incubation for 30 min at 37°C (grey) compared to 4°C (black).

Remaining surface-bound antibody was detected in flow cytometry. MFI was normalized to control human IgG1 binding. MFI= mean fluorescence intensity. Unpaired, two-tailed Student's t-test; *p<0.05; mean ± s.d. of n=3 is depicted. (D) Cell surface binding of 20D9 mab or control human IgG1 antibody to Ba/F3 cells stably expressing pMIY (Ba/F3-pMIY) empty vector (ev), human wildtype (hFLT3wt) or ITD mutant human FLT3 (hFLT3ITD) was measured in flow cytometry. Mean ± s.d. of n=3. (E) Temperature induced internalization of 4B12 mab in MOLM-13 (FLT3 positive) cells after 30 min incubation at 37°C compared to 4°C and HL-60 (FLT3 negative) after 37°C incubation assessed in immunofluorescence staining. Red = FLT3 staining by 4B12, Green = membrane staining by Vybrant DiO, Blue = nuclear staining by DAPI. Scale bar 5 µm. Representative pictures are shown. (F) Cell surface binding of 20D9 mab or control hIgG1 antibody to Ba/F3-pMIY ev, hFLT3wt, murine (mFLT3wt) or cynomolgues monkey FLT3 (cynoFLT3wt) was measured in flow cytometry. Mean ± s.d. of n=3. (G) Cell surface binding of 20D9 mab or control hIgG1 antibody to Ba/F3-pMIY ev, hFLT3wt or epitope mutant FLT3 (hFLT3/S50P/P54R) measured in flow cytometry. Mean ± s.d. of n=3. (H) Cell surface binding of 20D9 mab or control hIgG1 antibody to Ba/F3-pMIY ev, hFLT3wt or human CD64 (hCD64) measured in flow cytometry. Mean ± s.d. of n=3.

Figure 2: Analysis of cytotoxicity of FLT3-specific 20D9-ADC to different FLT3 variants.

(A) Schematic process of P5 conjugation technology[37] via disulfite bond reduction and Staudinger induced Michael addition. Final ADC consists of monoclonal antibody (20D9 or IgG1 antibody) coupled to monomethyl auristatin F toxin. Figure was created with BioRender.com. (B-E,G) Assessment of cytotoxicity of ADCs in different Ba/F3 cell lines. Viability was determined after 72 h treatment with different ADC concentrations by trypan blue exclusion count and compared to untreated control. Mean ± s.d. of n=3 biological replicates. (B) Treatment of Ba/F3-pMIY ev, hFLT3wt and hFLT3ITD cells with 20D9-ADC. (C) Treatment of Ba/F3-pMIY ev, hFLT3wt, mFLT3wt and cynoFLT3wt cells with 20D9-ADC. (D) Treatment of Ba/F3-pMIY ev, hFLT3wt and hFLT3/S50P/P54R cells with 20D9-ADC. (E) Treatment of Ba/F3-pMIY ev or hCD64 with either 20D9-ADC or IgG1-ADC. (F) IC50 values of 20D9-ADC and IgG1-ADC in Ba/F3-CD64 and Ba/F3-CD64-FLT3 cells. Calculation based on data from Figure 2E and 2G calculated by GraphPad Prism. Unpaired, two-tailed Student's t-test; *p<0.05. Each dot represents a replicate, horizontal line indicates mean. (G) Treatment of Ba/F3-pMIY ev or hCD64 and hFLT3 (CD64-FLT3) with different concentrations of either 20D9-ADC or IgG1-ADC.

Figure 3: Analysis of 20D9-ADC and control IgG1-ADC cytotoxicity in leukemia and lymphoma cell lines.

(A) Correlation of MFI of CD64 cell surface expression and MFI of FLT3 cell surface expression of myeloid human cell lines measure in flow cytometry. Expression data presented in Supplementary Figure 5A and B. Black line indicates simple linear regression with error interval. r= Pearson correlation coefficient; r^2= Coefficient of determination; p= p value from two tailed test with confidence interval of 95%. MFI= mean fluorescence intensity. (B,C,E,F) Assessment of cytotoxicity of ADCs in different human cell lines. Viability was determined after 96h treatment with different concentrations of ADCs by resazurin fluorescence and normalized to untreated control. Dashed line indicates 100 ng/ml drug concentration. Mean ± s.d. of n=3 biological replicates. (B) Treatment of FLT3 positive human cell lines with 20D9-ADC. (C) Treatment of FLT-3 negative human cell lines with 20D9-ADC. (D) Correlation of IC50 values of 20D9-ADC and sum of MFI of FLT3 and CD64 cell surface expression of myeloid human cell lines measure in flow cytometry. Expression data presented in Supplementary Figure 5 A,B and IC50 values of

20D9-ADC in Supplementary Table 1. Black line indicates simple linear regression with error interval. (E) Treatment of FLT3 positive human cell lines with IgG1-ADC. (F) Treatment of MOLM-13 cells with either native, buffer-incubated control (buffer control), or deglycosylated (deglyc.) 20D9-ADC or IgG1-ADC.

Figure 4: Evaluation of *in vivo* activity of 20D9-ADC in xenograft mouse models.

NSG mice were injected intravenously (i.v.) with $1x10^5$ luciferase expressing MOLM-13 cells (A-C) or $2x10^6$ luciferase expressing AML-573 PDX cells (D,E). Leukemic burden was monitored once or twice a week by bioluminescence imaging (BLI), and total flux was quantified. Mean $\pm$ s.d. is depicted. Treatment is indicated with rectangles in dark blue (20D9-ADC, 3 mg/kg), light blue (20D9-ADC, 1 mg/kg), grey (PBS) or black (all groups as indicated). (A) One week after transplantation, mice were treated with 20D9-ADC (1 mg/kg or 3 mg/kg, i.v.) or PBS as control (n=4/group) once a week for six weeks (1 mg/kg) or for four weeks (3 mg/kg). (B) BLI pictures of one representative mouse per group are shown. (C) One week after transplantation, mice were treated with either native or glycosylated 20D9-ADC or with either native or glycosylated IgG1-ADC (3 mg/kg; n=3/group) once a week for two weeks. PBS control mice of experiment shown in A are included as control. (D) FLT3 RNA expression of AML PDX samples (n=21) and primary patient samples[39] (n=261) analyzed by SCRB sequencing[61]. Data presented as normalized log2 counts per million (cpm). Samples selected for *ex vivo* and *in vivo* analysis are marked in blue. (E) 20 days after transplantation, mice were treated at intermediate tumor burden with 20D9-ADC (3 mg/kg) or PBS as control (n=3/group) once a week for up to four weeks (2 mice) or five weeks (one mouse). (F) PBS-treated control mice from (E) (n=3) were treated at day 41 after transplantation at advanced tumor burden with 20D9-ADC once a week for four weeks (two doses of 3 mg/kg, followed by two doses of 1 mg/kg).

Figure 5: Analysis of hematotoxicity of 20D9-ADC.

(A) Expression of FLT3 and CD64 in CD34 positive healthy bone marrow (BM) cells measured in flow cytometry. Mean ± s.d. of n=3 donors. (B,C) CD34 positive cells were treated with 0.04 µg/ml, 0.2 µg/ml or 1 µg/ml 20D9-ADC, 1 µg/ml IgG1-ADC or PBS and analyzed in flow cytometry after 4 days. Kruskal-Wallis test; *p<0.05; **p<0.01; ***p<0.001; Mean ± s.d. of n=5. (B) Percentage of living cells measured with Annexin V/PI staining and normalized to PBS. (C) Differentiation assessment after staining to differentiation markers. CMP: common myeloid progenitors; GMP: granulocyte-monocyte progenitors; MEP: megakaryocyte/erythroid progenitors; MLP: multilymphoid progenitors; MPP: multipotent progenitors; hematopoietic stem cells (HSC). (D) Assessment of clonogenic capacity of healthy CD34+ BM cells. Cells were treated with 0.04 µg/ml, 0.2 µg/ml or 1 µg/ml 20D9-ADC, 1 µg/ml IgG1-ADC or PBS and plated afterwards for colony forming unit (CFU) assay without further treatement. After 14 days, colonies were counted. GEMM: granulocyte, erythrocyte, macrophage, megakaryocyte. GM: granulocyte, macrophage. M: macrophage. G: granulocyte. E: erythrocyte. BFU-E: burst-forming unit erythrocyte. 2way ANOVA; *p<0.05; Mean ± s.d. of n=5.

Figure 6: Treatment combination of 20D9-ADC and tyrosine kinase inhibitors.

(A,B) Upregulation of FLT3 cell surface expression in MOLM-13 cells after treatment with kinase inhibitors compared to untreated control. Cells were analyzed in flow cytometry after treatment. Dotted line represents MFI ratio of untreated cells. Mean ± s.d. of n=2 is depicted. (A) Cells were

716 treated with 5, 25 or 50 nM midostaurin, quizartinib and sorafenib for 6, 24, 48 or 72 h. (B) Cells
717 were treated with 5 nM midostaurin, 1 nM quizartinib, 5 nM sorafenib or 1 μM dasatinib for 72
718 h. (C-F) Treatment combination of 20D9-ADC and midostaurin (C,D) or quizartinib (E,F) in
719 MOLM-13 cells compared to treatment with 20D9-ADC, midostaurin or quizartinib as single
720 agent. Viability was determined after 96h by resazurin fluorescence and normalized to dimethyl
721 sulfoxide (DMSO) treated control. (C,E) Each dot represents one biological replicate, the
722 horizontal line indicates the mean. two-way ANOVA; *p<0.05; **p<0.01; ***p<0.001.
723 Combination indices (CIs) with standard deviation were determined using CompuSyn software;
724 CI < 1 indicates synergy and is underlined; CI = 1 additivity; CI > 1 antagonism. (D,F) The
725 synergy score was calculated by 'Synergy Finder' software using zero interaction potency (ZIP)
726 modeling. Grey triangles indicate increasing drug concentrations. A positive Synergy score value
727 δ and the red coloring indicate synergism. (G) Treatment combination of 20D9-ADC and
728 midostaurin *in vivo*. NSG mice were injected i.v. with 1e5 luciferase expressing MOLM-13 cells.
729 Leukemic burden was monitored once or twice a week by BLI, and total flux was quantified.
730 Mean ± s.d. is depicted. One week after transplantation, mice were treated for three weeks with
731 20D9-ADC (1 mg/kg i.v., once per week), midostaurin (50 mg/kg p.o. 5 days a week), a
732 combination of both or PBS as control (n=4/group). Bioluminescence imaging of one
733 representative mouse of each group at day 6 and 16.

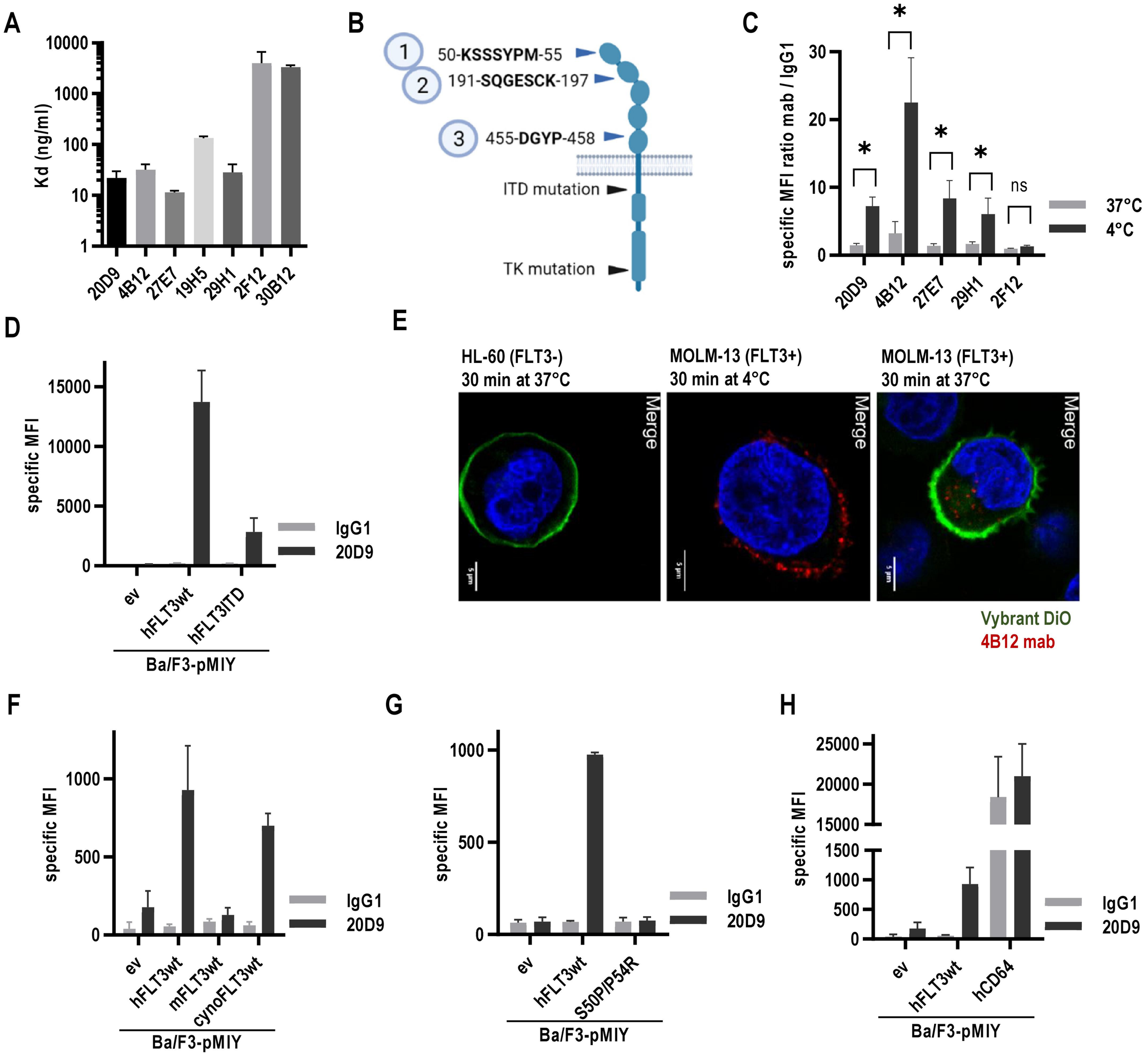

Figure 1: Evaluation of epitope specificity and internalization of anti-FLT3 monoclonal antibodies.

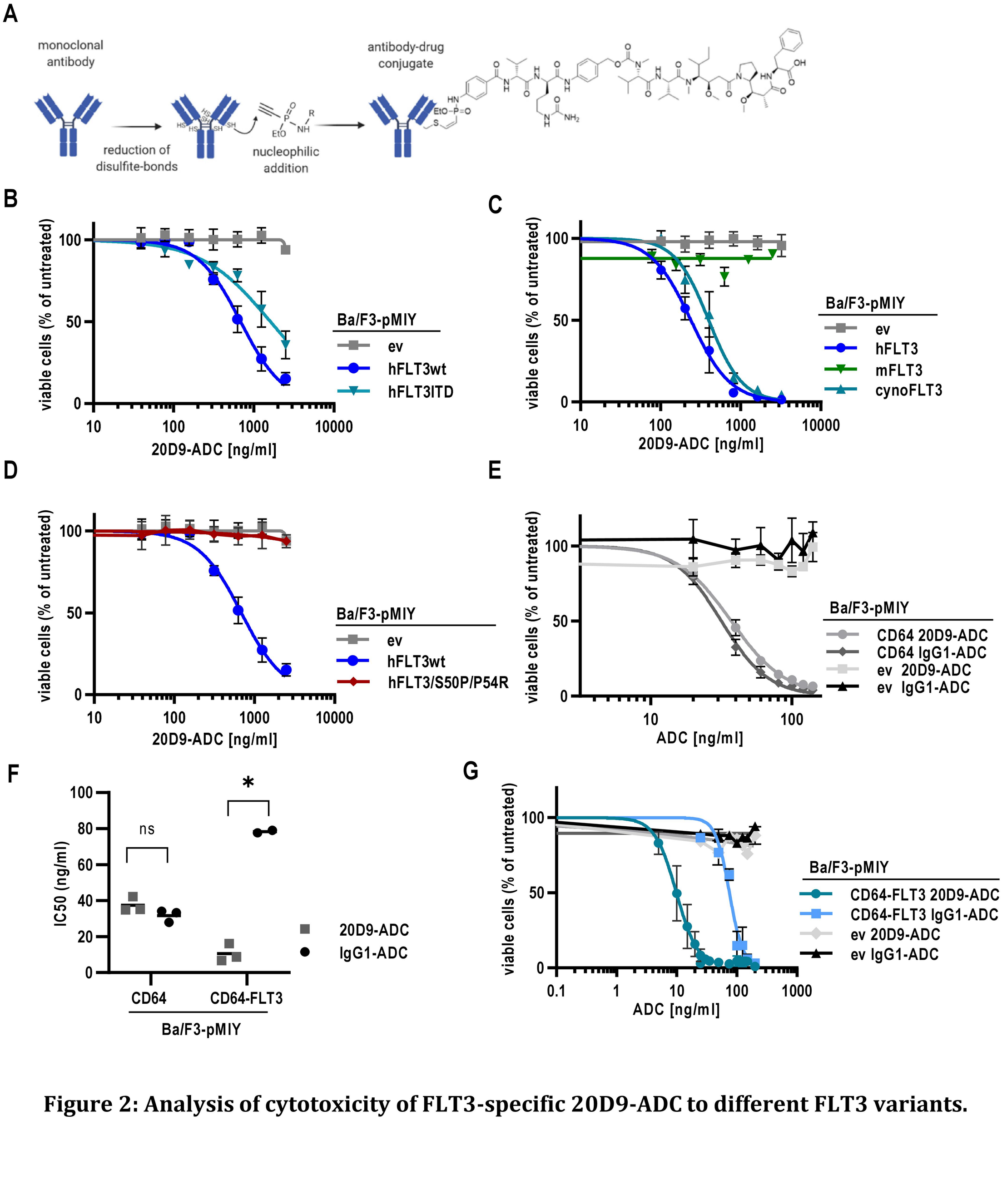

Figure 2: Analysis of cytotoxicity of FLT3-specific 20D9-ADC to different FLT3 variants.

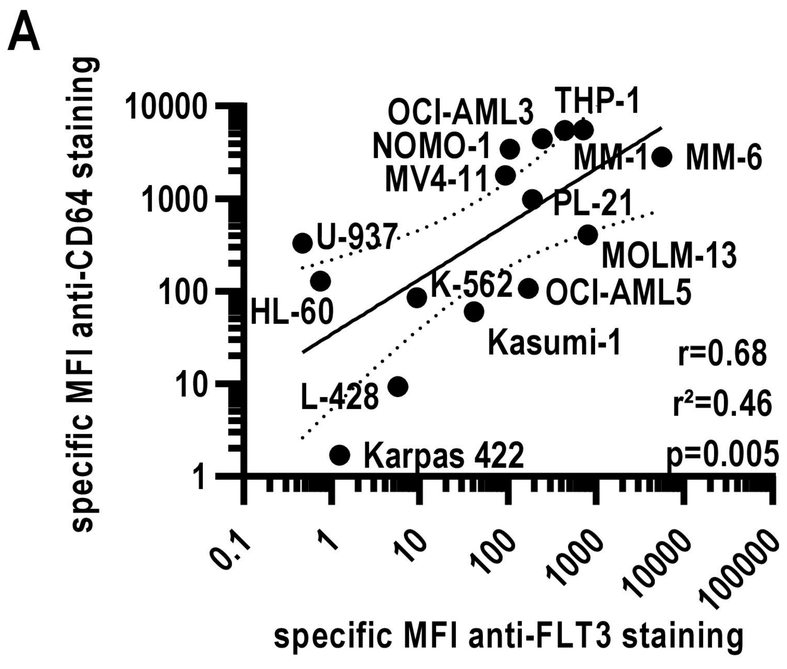

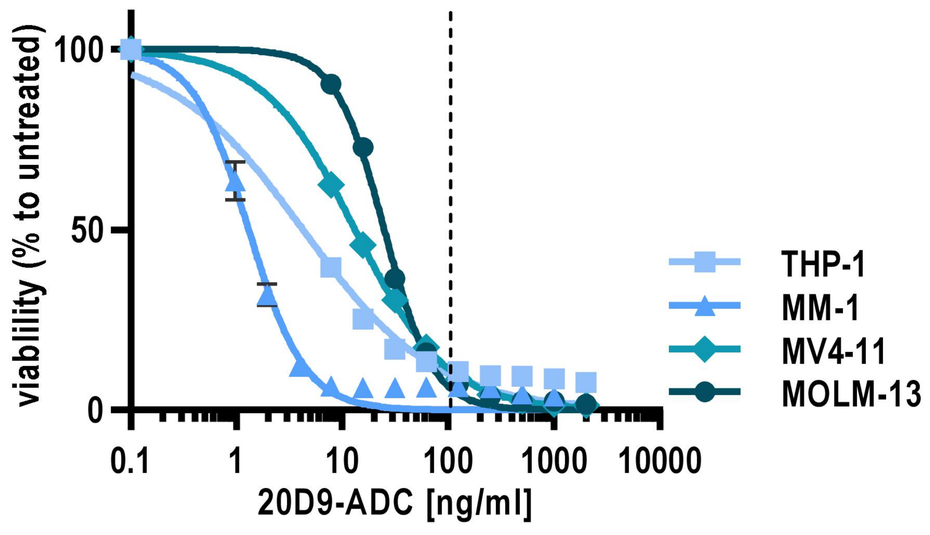

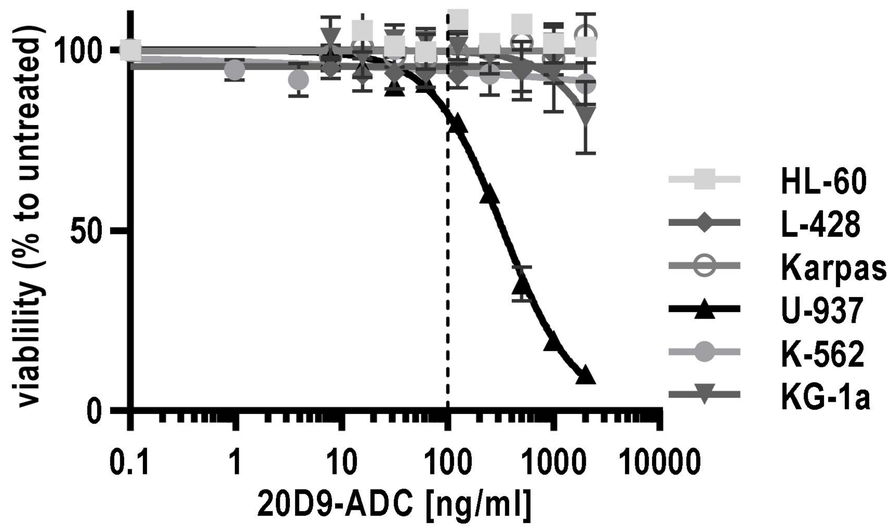

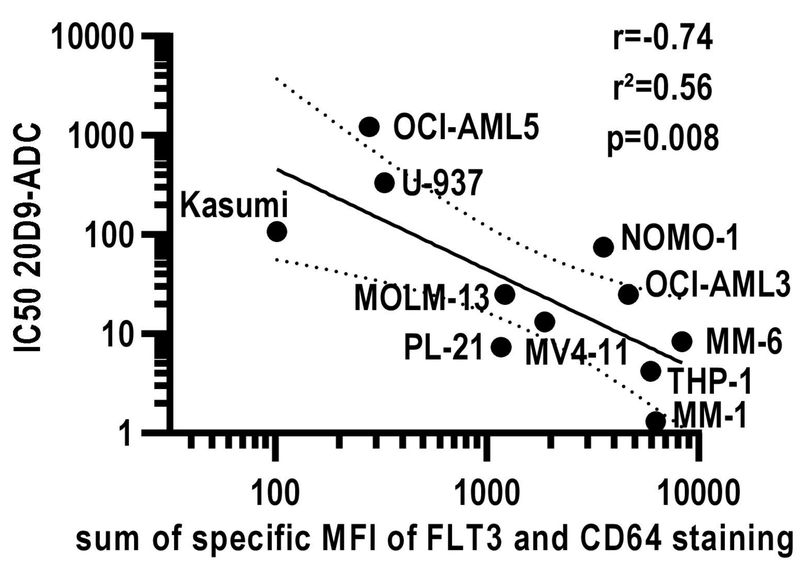

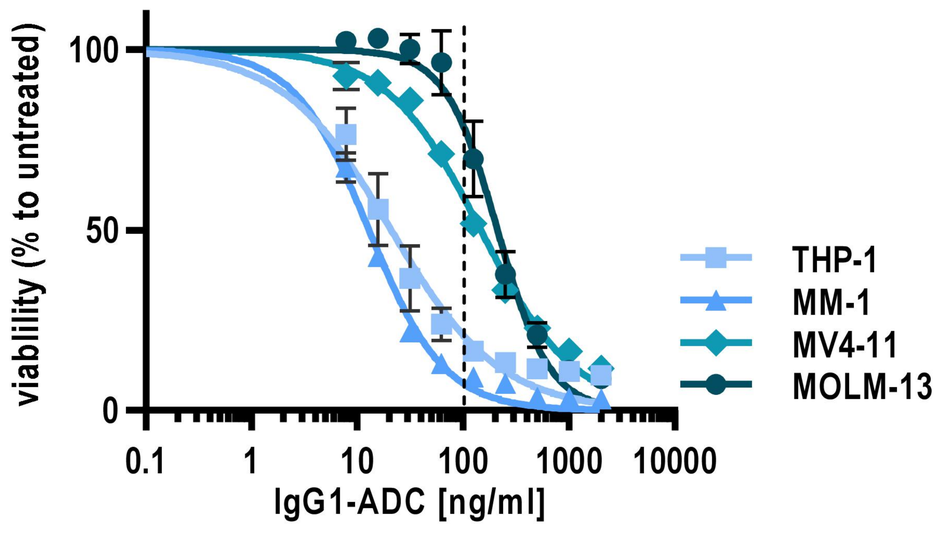

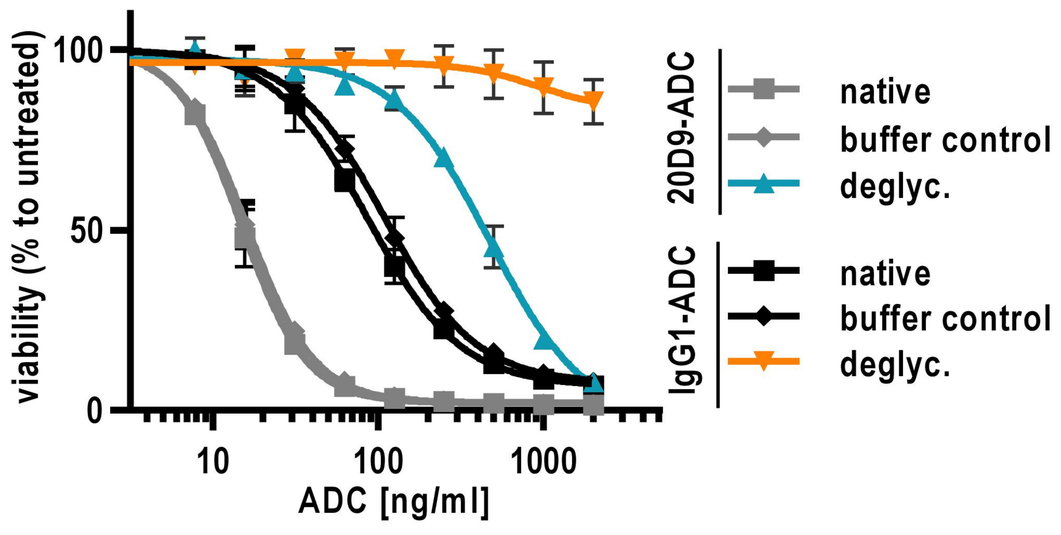

IC50 (ng/ml)	control	deglyc.
20D9-ADC	15.7	473.7
IgG1-ADC	102.2	>2000

Figure 3: Analysis of 20D9-ADC and control IgG1-ADC cytotoxicity in leukemia and lymphoma cell lines.

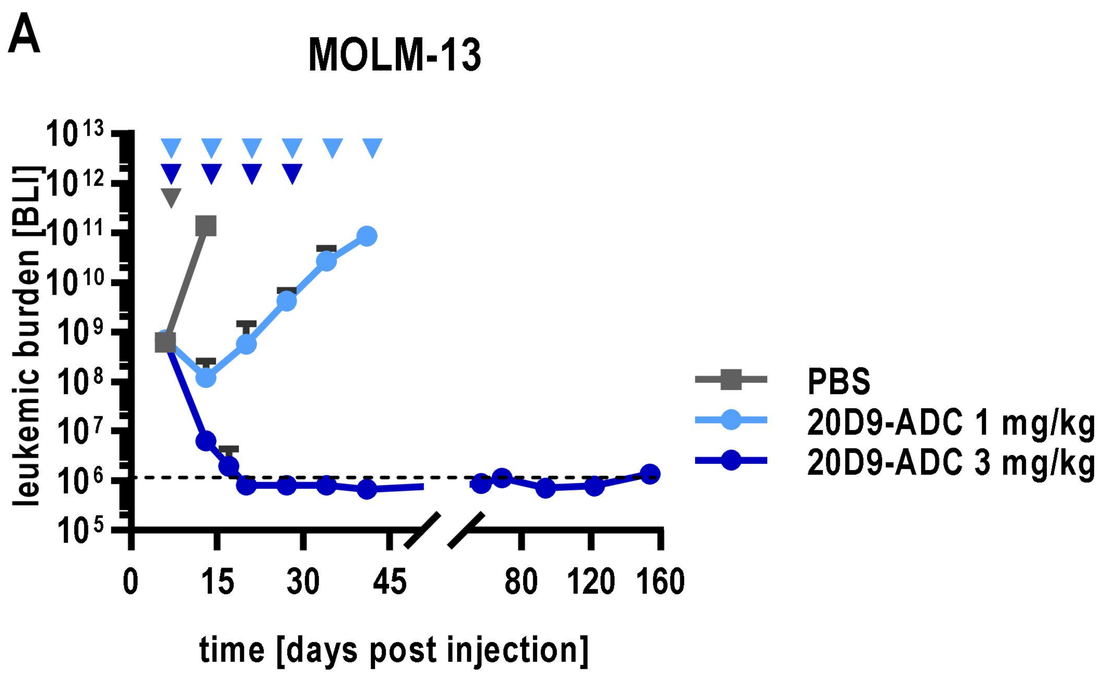

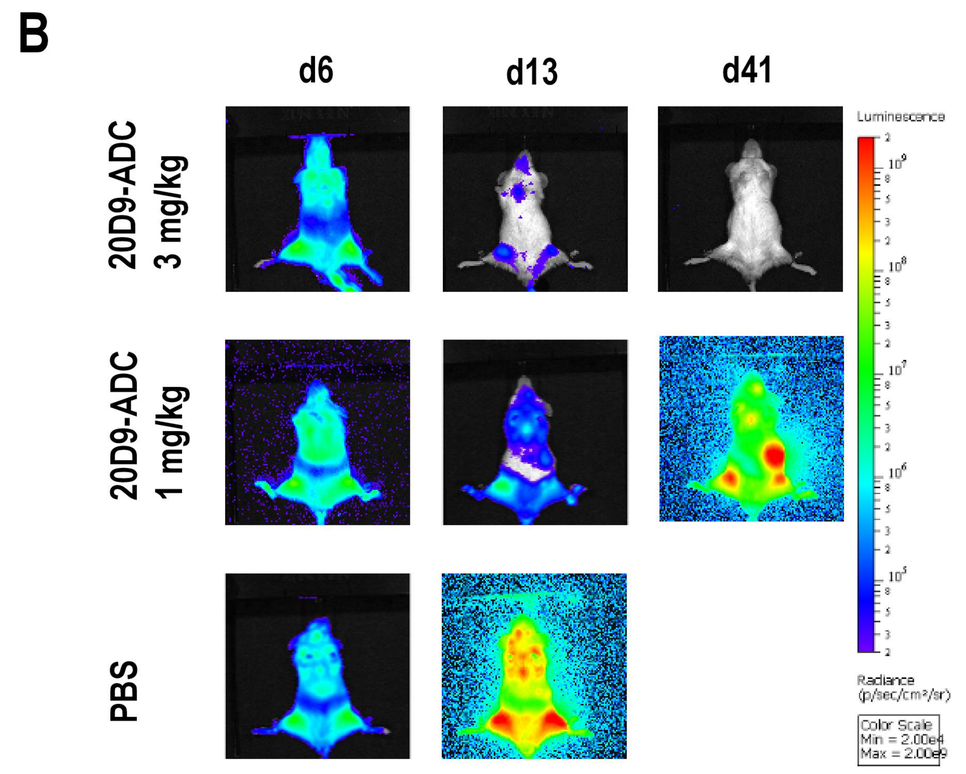

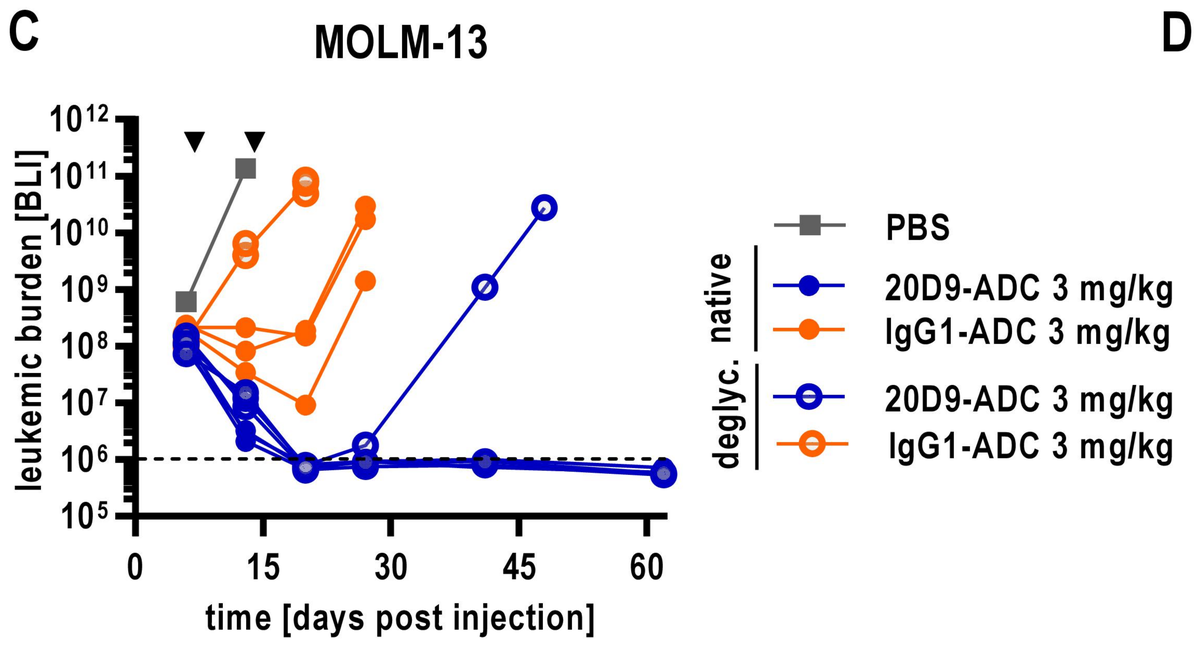

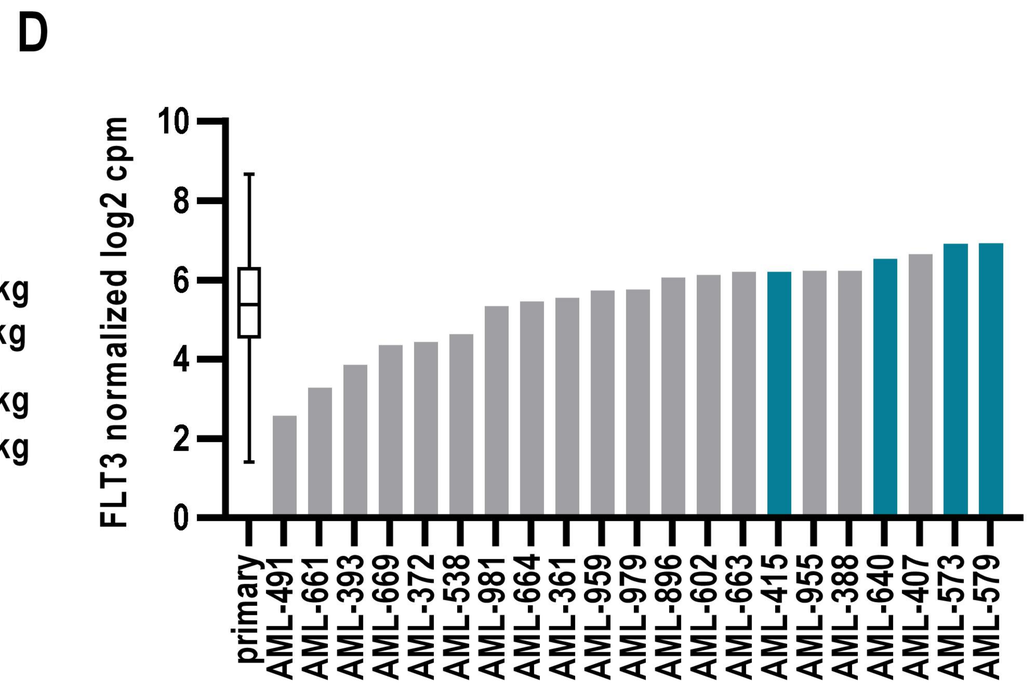

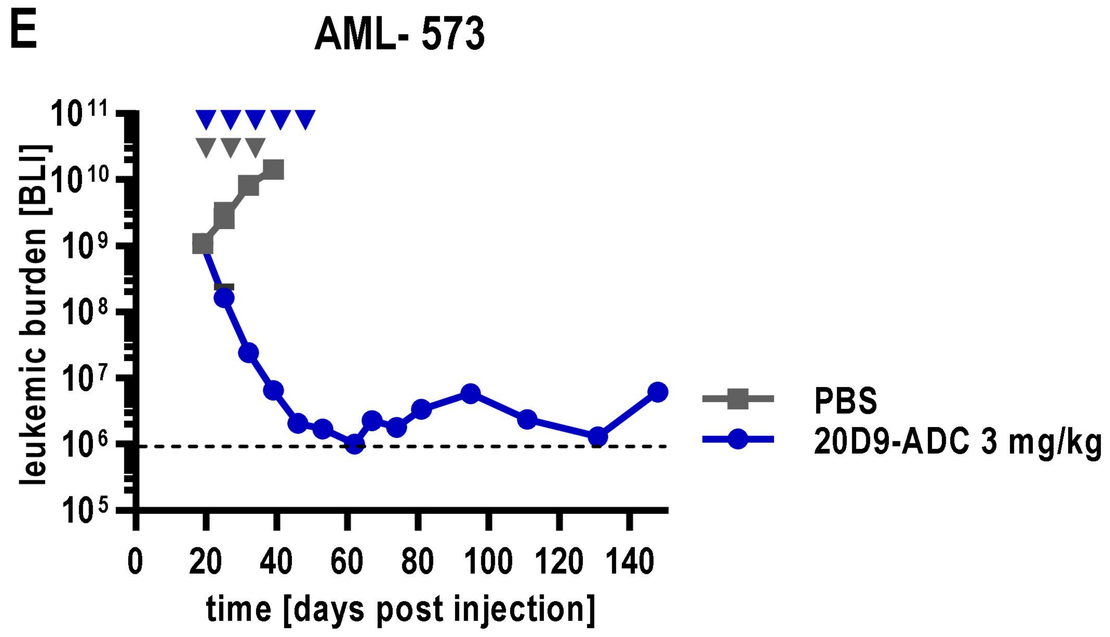

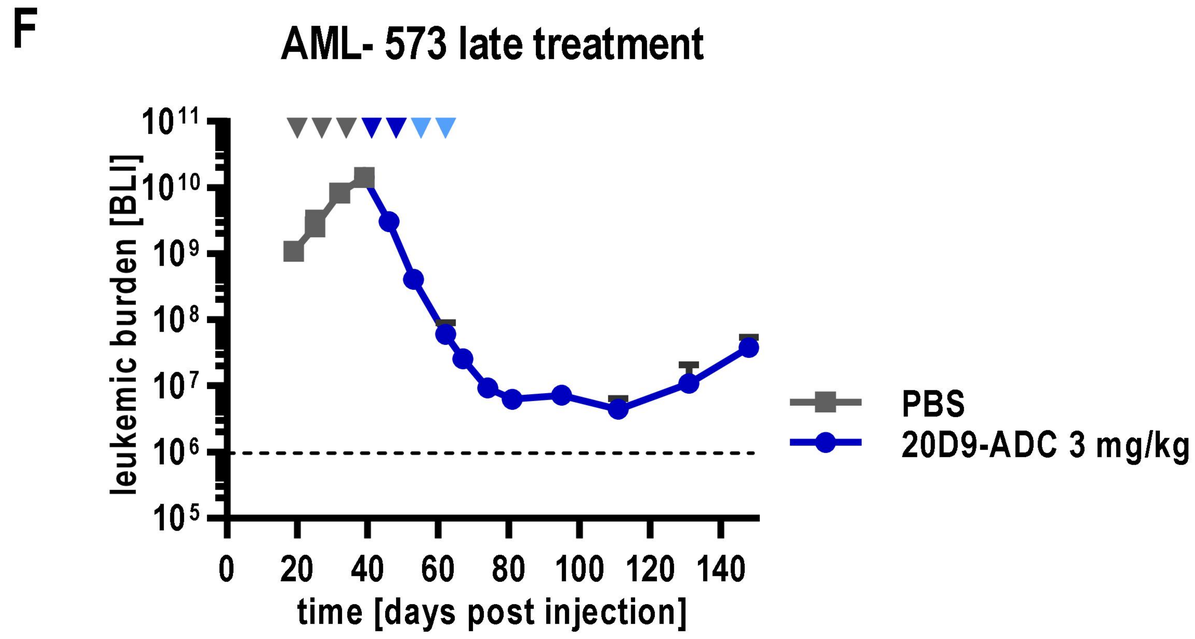

Figure 4: Evaluation of *in vivo* activity of 20D9-ADC in xenograft mouse models.

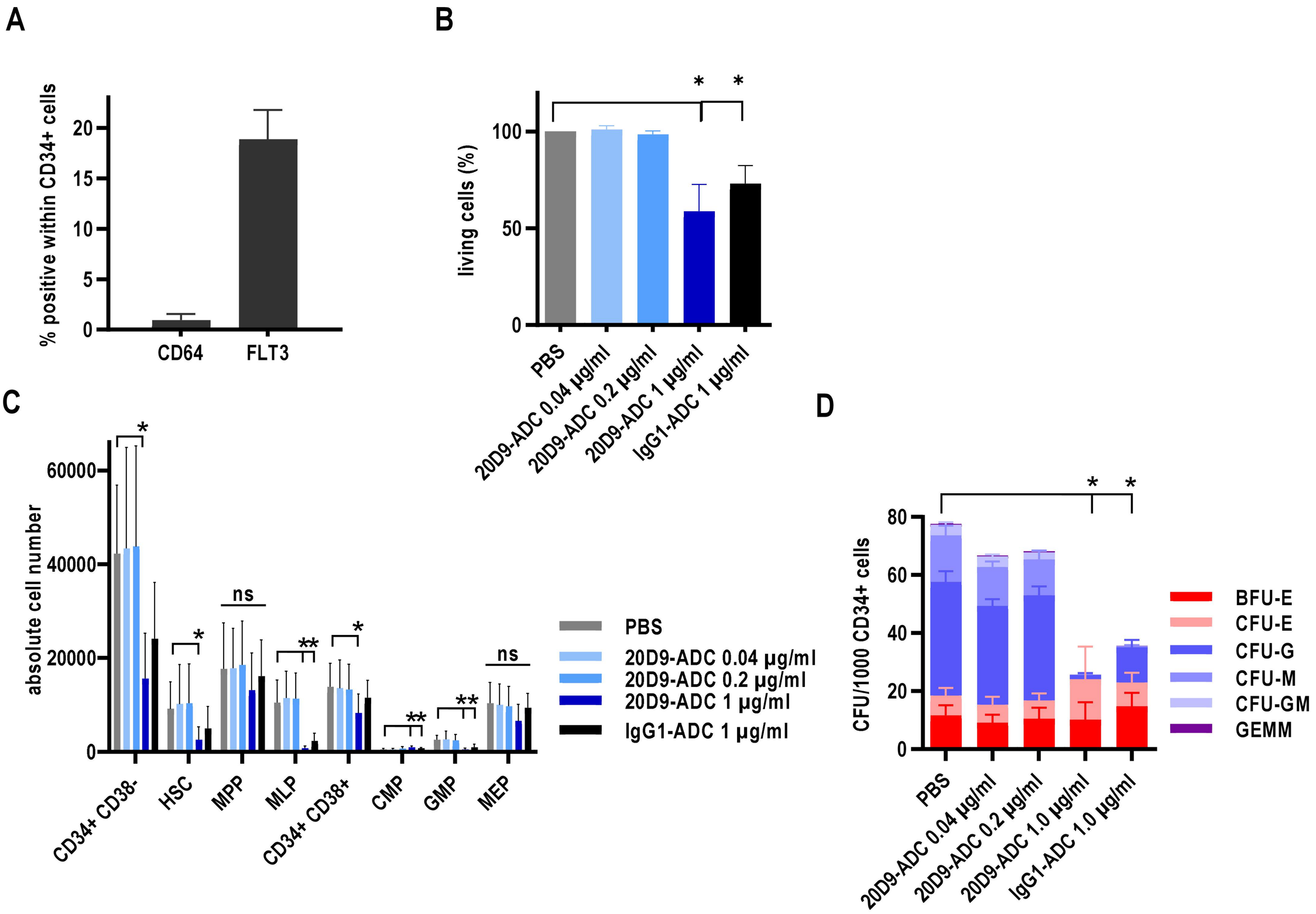

Figure 5: Analysis of hematotoxicity of 20D9-ADC.

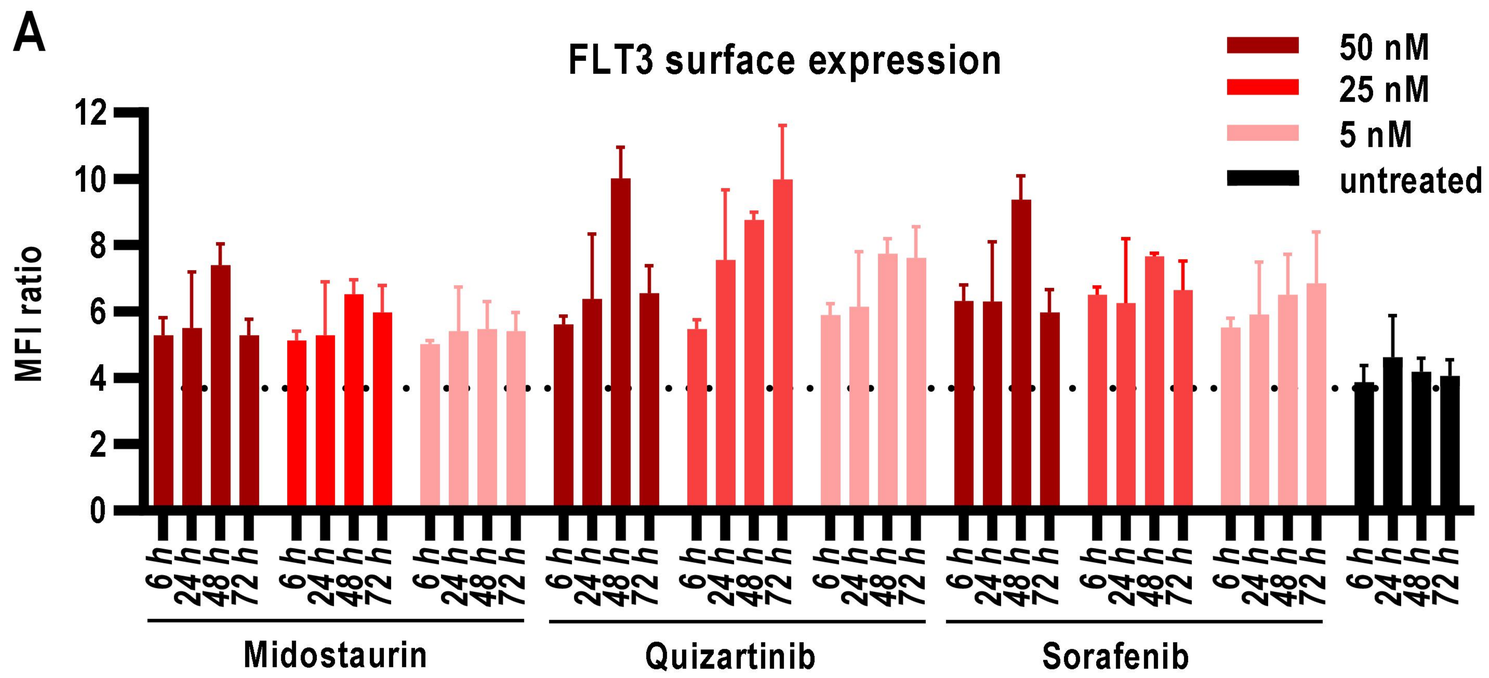

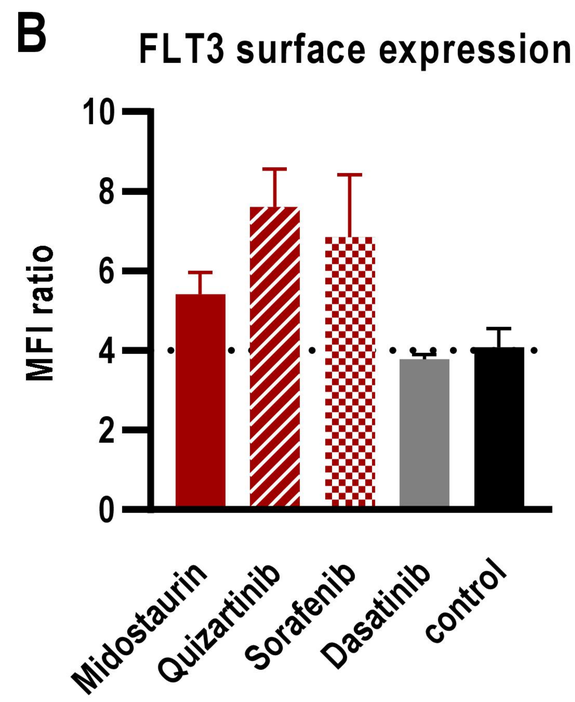

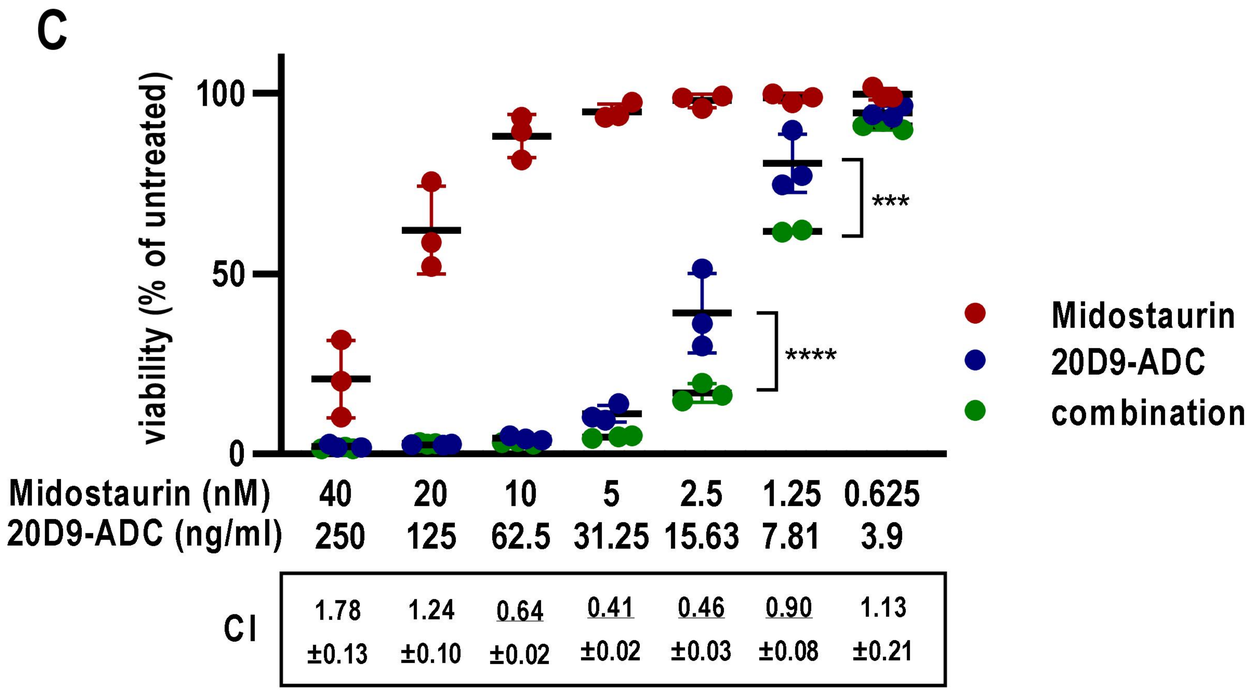

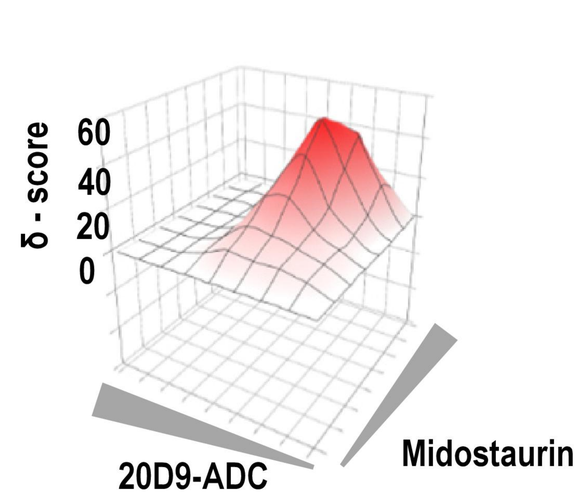

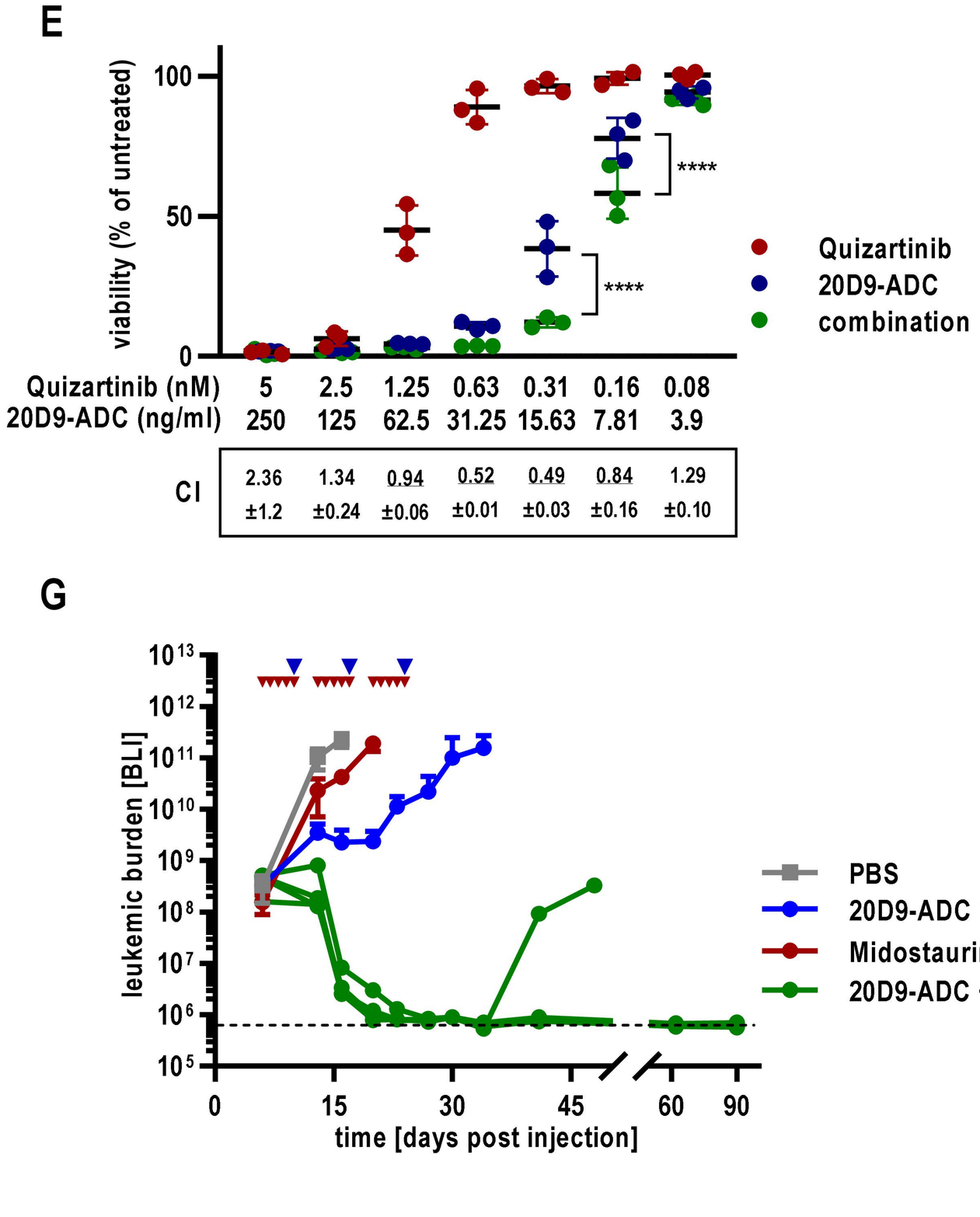

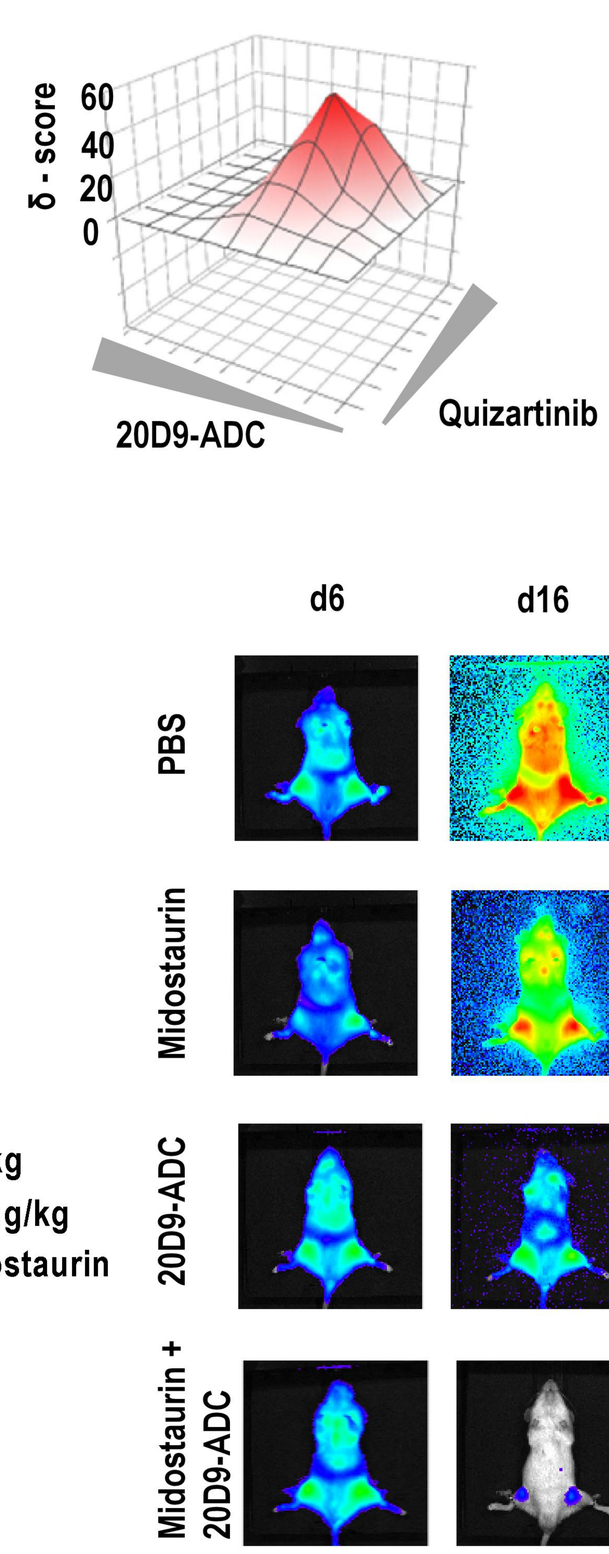

Figure 6: Treatment combination of 20D9-ADC and tyrosine kinase inhibitors.